

Forward hysteresis and Hopf bifurcation in an NPZD model with application to harmful algal blooms

J. C. Macdonald^{1,2*} and H. Gulbudak^{1*}

¹Department of Mathematics, University of Louisiana at Lafayette, 1401 Johnston Street, Lafayette, 70504, Louisiana, USA.

²Current address: School of Zoology, Faculty of Life Sciences, Tel Aviv University, Tel Aviv-Yafo, Israel.

*Corresponding author(s). E-mail(s): joshuamac@tauex.tau.ac.il;
hayriye.gulbudak@louisiana.edu;

Abstract

Nutrient-Phytoplankton-Zooplankton-Detritus (NPZD) models, describing the interactions between phytoplankton, zooplankton systems, and their ecosystem, are used to predict their ecological and evolutionary population dynamics. These organisms form the base two trophic levels of aquatic ecosystems. Hence understanding their population dynamics and how disturbances can affect these systems is crucial. Here, starting from a base NPZ modeling framework, we incorporate the harmful effects of phytoplankton overpopulation on zooplankton - representing a crucial next step in harmful algal bloom (HAB) modeling - and split the nutrient compartment to formulate an NPZD model. We then mathematically analyze the NPZ system upon which this new model is based, including local and global stability of equilibria, Hopf bifurcation condition, and forward hysteresis, where the bi-stability occurs with multiple attractors. Finally, we extend the threshold analysis to the NPZD model, which displays both forward hysteresis with bi-stability and Hopf bifurcation under different parameter regimes, and examine ecological implications after incorporating seasonality and ecological disturbances. Ultimately, we quantify ecosystem health in terms of the relative values of the robust persistence thresholds for phytoplankton and zooplankton and find (i) ecosystems sufficiently favoring phytoplankton, as quantified by the relative values of the plankton persistence numbers, are vulnerable to both HABs and (local) zooplankton extinction (ii) even healthy ecosystems are extremely sensitive to nutrient depletion over relatively short time scales.

Keywords: plankton population dynamics, eutrophication, reoligotrophication, harmful algal blooms

1 Introduction

Plankton are a ubiquitous group of very small drifting organisms which live in both salty and fresh water and form the base trophic levels of aquatic food webs [1]. Divided by trophic position, phytoplankton are primary producers, generating growth through photosynthesis, while zooplankton are primary consumers, and feed primarily on phytoplankton [1]. Mixotrophic organisms, those which can opportunistically switch between photosynthesis and heterotrophy, also exist in this group [2, 3]. Disturbance is an important mechanism that affects the functioning of these ecosystems, and variation in type, frequency, intensity, and duration of disturbance has important implications for ecosystem and community structure and thus underlying population dynamics [4]. There is general agreement that a high frequency of ecological disturbance has a net negative effect on ecosystem species diversity [5]. Given plankton's foundational position in aquatic food webs, understanding their interactions and population dynamics is a central focus in aquatic ecology (cf [6–8]) - not least because they can be main drivers of knock-on effects of ecological disturbances. Here we focus in particular on plankton population dynamics in the wake of nutrient influx (eutrophication, [9, 10]) and nutrient depletion events (re-oligotrophication, see [11]), which are of immediate concern given their potential cascading cross-scale knock-on effects which can range from local die-offs [12], to diverse disease spillover events and pathogenesis of vector-borne disease (particularly in freshwater ecosystems, [13–15]), and that under the current climate regime, conditions that promote their occurrence have been both predicted to and shown to increase ([9–11, 16]) in contrast to other potential disturbances.

Plankton blooms are naturally occurring in temperate zones during the spring [1]. However, phytoplankton blooms may cause deleterious ecological effects through toxicity (e.g., harmful algal blooms (HABs) or through the formation of low oxygen/hypoxic zones, cf [17–19]), both of which negatively affect ecological consumers (e.g., zooplankton or fishes; [9, 10, 20]). There is debate about what exactly is classified as a bloom versus what is not (but see [21] for one definition). Here, we take a conservative approach and say a bloom has occurred if the peak phytoplankton concentration is at least 300% the mean value of the time simulation over the course of one year, and investigate their effects as a disturbance of plankton population dynamics.

Nutrient-Phytoplankton-Zooplankton-Detritus (NPZD) models (cf. [22–29]) have long been used by plankton ecologists to investigate plankton interactions and long-term population dynamics in various settings from lakes to the far-from-shore ocean. These models are essentially nested Lotka-Volterra models with phytoplankton ‘predating’ nutrients and zooplankton predating phytoplankton and are used to study the mechanisms that sustain plankton coexistence and diversity [26, 27]. Hopf bifurcation, which biologically corresponds to predator-prey feedback loops, is a common

feature of these models (cf. [23, 25]), and forward hysteresis has been demonstrated depending on the choice of zooplankton mortality term [25]. Nutrient cycling has also been modeled by incorporating delay differential equations instead of a separate detritus compartment [29]. However, many of these models - particularly those with many nonlinear terms - have not been mathematically analyzed, which is crucial for understanding complex interactions between NPZ(D) systems, and have not been used in the context of ecological disturbances.

In this study, starting from a base NPZ modeling framework from the literature [24, 25], we incorporate the harmful effects of phytoplankton overpopulation on zooplankton by adding a functional form to the zooplankton compartment and split the nutrient compartment to formulate an NPZD model (Section 2). To our best knowledge, this is the first multi-trophic level model to incorporate process-based effects of harmful algal blooms (HABs), which has been argued for as a crucial next step in HAB modeling [20]. We then mathematically analyze the NPZ system upon which this new model is based with both quadratic and linear zooplankton mortality terms (Section 3) - deriving global stability conditions for the zooplankton extinction equilibrium in terms of zooplankton invasion number for a special case of the linear mortality model. We also derive local stability, Hopf bifurcation, and derive existence conditions for the coexistence equilibria of the NPZ model with both quadratic and linear zooplankton mortality. We also provide one and two-parameter bifurcation diagrams for both models, showing forward hysteresis with bi-stability or Hopf bifurcation in the quadratic loss case depending on parameter values, along with Hopf bifurcation or transcritical bifurcation in the linear loss case. Finally, we extend the threshold analysis to the new NPZD model, which displays both forward hysteresis with bi-stability and Hopf bifurcation, and examine ecological implications after incorporating seasonality and ecological disturbances in the form of eutrophication and re-oligotrophication events (Section 4). Ultimately we quantify ecosystem health in terms of the relative values of the robust persistence thresholds for phytoplankton and zooplankton and find (i) ecosystems sufficiently favoring phytoplankton are vulnerable to both HABs and (local) zooplankton extinction (ii) even balanced ecosystems are extremely sensitive to nutrient depletion over relatively short time scales.

2 Modeling NPZ and NPZD systems

The general form of the coupled nonlinear NPZ ODE models describes the interactions between nutrients (N), phytoplankton (P), and zooplankton (Z). The terms $f(P), g(N)$ represent phytoplankton's response to light (ie. growth), and phytoplankton nutrient uptake, respectively. The terms $h(P), i(P)$ denote phytoplankton mortality due to zooplankton grazing, and natural mortality, respectively. Zooplankton growth is driven by interaction with phytoplankton, scaled by zooplankton assimilation, which can be thought of as 'messy eating'. Because zooplankton are the highest trophic level modeled, all zooplankton loss is generally accounted for with a single functional form, $j(Z)$. In addition to nutrient loss due to phytoplankton nutrient uptake, nutrient loss/exchange can also occur due to other factors such as re-oligotrophication [11] or cross-thermocline exchange of nutrients [22], which is represented by the functional

term $m(N)$. Furthermore, nutrient growth results from plankton death and inefficient zooplankton grazing, denoted with the term $(1 - \gamma)h(P)Z$, where γ represents the zooplankton assimilation rate. The general form of the NPZ model is given as follows [27] (see schematic Figure 1):

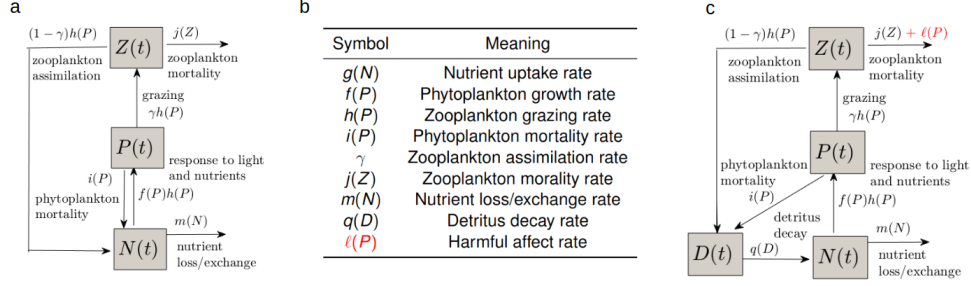


Fig. 1: The general NPZ and NPZD modeling framework (a) The general NPZ model **(b)** Table with a description of model transition rates. **(c)** The general NPZD model with new functional form, $\ell(P)$, highlighted in red.

$$\begin{cases} \dot{P} = f(P)g(N)P - h(P)Z - i(P)P, \\ \dot{Z} = \gamma h(P)Z - j(Z)Z, \\ \dot{N} = -f(P)g(N)P + (1 - \gamma)h(P)Z + i(P)P - m(N). \end{cases} \quad (1)$$

Following [24, 25], we consider the specific functional forms:

$$\begin{aligned} f(P) &= \beta \left(1 - \frac{P}{K}\right), \quad g(N) = \frac{N}{k + N}, \quad h(P) = \frac{\eta P^2}{\mu^2 + P^2}, \\ j(Z) &= \delta Z^\sigma, \quad i(P) = 0, \quad m(N) = S(N - \Theta). \end{aligned} \quad (2)$$

Therefore one can obtain the following coupled ODE model:

$$\begin{cases} \dot{P} = \frac{N}{k + N} \beta P \left(1 - \frac{P}{K}\right) - \frac{\eta P^2}{\mu^2 + P^2} Z, \\ \dot{Z} = \gamma \left[\frac{\eta P^2}{\mu^2 + P^2} - \delta Z^\sigma \right] Z, \\ \dot{N} = -\beta \frac{N}{k + N} \left(1 - \frac{P}{K}\right) P + (1 - \gamma) \frac{\eta P^2}{\mu^2 + P^2} Z - S(N - \Theta) \end{cases} \quad (3)$$

In the NPZ model (3), the modified logistic equation for phytoplankton growth has the saturating response of Holling's type II for nutrient uptake (Michaelis-Menten kinetics). We also have a saturating response of Holling's type III function for the zooplankton grazing of phytoplankton [30]. These are chosen because plankton are known to not have well-mixed spatial distributions [22]. The parameters k, K, η and

μ denote the Michaelis-Menton half saturation constant, the phytoplankton carrying capacity, the maximum zooplankton grazing rate, and the half-saturation grazing constant, respectively. Zooplankton growth is in direct response to interaction with phytoplankton, scaled by the zooplankton assimilation rate, γ , and loss is assumed to be either linear ($\sigma = 0$) or quadratic ($\sigma = 1$) with death rate δ . Moreover, the parameter S represents the nutrient loss/exchange rate. Finally, the parameter Θ represents the intrinsic nutrient level.

2.1 Incorporating harmful affect of phytoplankton overpopulation

To account for the harmful effect of phytoplankton overpopulation on zooplankton during harmful algal blooms, as well as nutrient cycling, we incorporate a new variable, $D(t)$, representing the amount of Detritus, to the model (1), providing a general NPZD framework (see Fig.1c) We then define the net reproductive rate of zooplankton as a function of phytoplankton as follows:

$$r(P) = \underbrace{h(P)}_{\text{zooplankton grazing}} - \underbrace{\ell(P)}_{\text{harmful affect of phytoplankton}}, \quad (4)$$

where $\ell(P) = \frac{\alpha P}{\Xi + P}$ with α representing the maximum harmful effect of phytoplankton on zooplankton, and Ξ denoting the half-saturation constant of the effect. The term $\ell(P)Z$ represents the deleterious effect of phytoplankton overpopulation on zooplankton. Additionally, to better capture nutrient cycling we split the compartment, \dot{N} , into two compartments, with \dot{D} representing the rate of change in detritus concentration which decays into nutrients at rate $q(D) = \Psi$, and phytoplankton having natural mortality rate $i(P) = \epsilon$.

This functional form of $r(P)$, given in (4), represents the beneficial effect of phytoplankton grazing for zooplankton population, and the deleterious effect of phytoplankton overpopulation on zooplankton. This formulation is motivated by our prior work, modeling antibody-dependent enhancement (ADE) in Dengue, where an increase in preexisting crossreactive antibodies can increase infection severity [31]. Here we assume that the net zooplankton reproduction can decrease as the phytoplankton population size P achieves a peak above some threshold, representing harmful bloom occurrence [9, 10] (see figure 2). Taken together this results in the model

$$\begin{cases} \dot{P} = \frac{N}{k + N} \beta P \left(1 - \frac{P}{K}\right) - \frac{\eta P^2}{\mu^2 + P^2} Z - \epsilon P, \\ \dot{Z} = \gamma \left(\left[\frac{\eta P^2}{\mu^2 + P^2} - \frac{\alpha P}{\Xi + P} \right] Z - \delta Z^2 \right), \\ \dot{N} = -\frac{N}{k + N} \beta P \left(1 - \frac{P}{K}\right) - S(N - \theta) + \Psi D \\ \dot{D} = (1 - \gamma) \frac{\eta P^2}{\mu^2 + P^2} Z + \epsilon P - \Psi D. \end{cases} \quad (5)$$

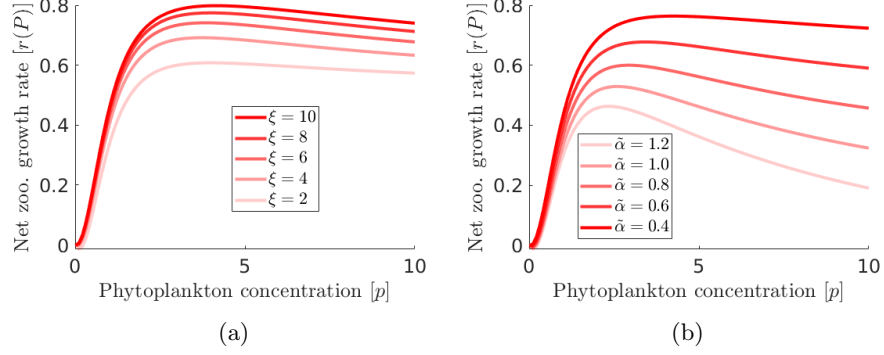


Fig. 2: The net zooplankton reproduction rate as a function of phytoplankton population. The precise shape of $r(P)$ is dictated by two rescaled model parameters: ξ and $\tilde{\alpha}$ (8), which represent the half-saturation constant and maximum harmful effect of phytoplankton on zooplankton respectively. In panel (a), the net zooplankton growth rate increases with ξ ($\tilde{\alpha}$ is fixed at 0.5), and in panel (b), it decreases as $\tilde{\alpha}$ increases (ξ is fixed at 5).

This model can be reparametrized via

$$\begin{cases} \tau = \beta t, p = \mu^{-1}P, z = \eta(\beta\mu)^{-1}Z, n = \mu^{-1}N, \\ a = \delta\beta\mu/\eta^2, s = S\beta^{-1}, \theta = \Theta\mu^{-1}, \\ \tilde{k} = k\mu^{-1}, c = K\mu^{-1}, \tilde{\gamma} = \eta\gamma\beta^{-1}, \end{cases} \quad (6)$$

similar to the NPZ models in [24, 25]. To further rescale new parameters in the model (5), we consider

$$\begin{cases} \tilde{\alpha} = \alpha\eta^{-1}, \xi = \Xi\mu^{-1}, d = D\mu^{-1} \\ \psi = \Psi\beta^{-1}, \tilde{\epsilon} = \epsilon\beta^{-1}, \end{cases} \quad (7)$$

Then the full NPZD model (5) can be re-scaled as:

$$\begin{cases} \frac{dp}{d\tau} = \frac{n}{\tilde{k} + n}p \left(1 - \frac{p}{c}\right) - \frac{p^2}{1 + p^2}z - \tilde{\epsilon}p \\ \frac{dz}{d\tau} = \tilde{\gamma} \left[\frac{p^2}{1 + p^2} - \frac{\tilde{\alpha}p}{\xi + p} - az \right] z \\ \frac{dn}{d\tau} = -\frac{n}{\tilde{k} + n}p \left(1 - \frac{p}{c}\right) - s(n - \theta) + \psi d \\ \frac{dd}{d\tau} = (1 - \gamma)\frac{p^2}{1 + p^2}z + \tilde{\epsilon}p - \psi d \end{cases} \quad (8)$$

In the system (8), the parameters a, s are respectively the rescaled zooplankton mortality and nutrient loss/exchange rates. Phytoplankton carrying capacity is represented by c , and $\tilde{\gamma}$ represents zooplankton assimilation scaled by the ratio of phytoplankton response to light, β , and maximum zooplankton grazing rate η .

3 Threshold analysis of the NPZ model

To understand the model dynamics and ecological impact of HABs, we first analyze the NPZ system (3) then we extend the analysis to the NPZD model (5) along with crucial ecological implications.

Note that the rescaled NPZ subsystem (3) is as follows [25]:

$$\begin{cases} \frac{dp}{d\tau} = \frac{n}{\tilde{k} + n} p \left(1 - \frac{p}{c}\right) - \frac{p^2}{1 + p^2} z \\ \frac{dz}{d\tau} = \tilde{\gamma} \left[\frac{p^2}{1 + p^2} - az^\sigma \right] z \\ \frac{dn}{d\tau} = -\frac{n}{\tilde{k} + n} p \left(1 - \frac{p}{c}\right) + (1 - \gamma) \frac{p^2}{1 + p^2} z - s(n - \theta) \end{cases} \quad (9)$$

For the analysis of the model (9), we consider two cases: (i) quadratic zooplankton loss term ($\sigma = 1$) and (ii) linear zooplankton loss term ($\sigma = 0$). All model parameters are assumed to be strictly positive. In both the case of a quadratic zooplankton loss term ($\sigma = 1$) and a linear zooplankton loss term ($\sigma = 0$), the model has two boundary equilibria in the positive phytoplankton-nutrient plane: $\mathcal{E}_{np} = (c, 0, \theta)$ and $\mathcal{E}_n = (0, 0, \theta)$.

For both of these equilibria, the steady state nutrient level is the intrinsic nutrient level of the system, θ . Equilibrium \mathcal{E}_{np} corresponds to the steady state with phytoplankton at their carrying capacity, c , and equilibrium \mathcal{E}_n represents community collapse. As we show below, changes in zooplankton loss term induce distinct qualitative dynamics. Regardless of the choice of zooplankton mortality functional form, the community collapse equilibrium is always unstable for this model.

Proposition 1. *The community collapse equilibrium, \mathcal{E}_n , of model (9) is always unstable.*

Proof. See appendix A. □

See Table 1 for a summary of results.

3.1 Linear zooplankton loss term ($\sigma = 0$) with the full model

Define the zooplankton invasion number,

$$\mathcal{R}_0 := \frac{1}{a} \cdot \frac{c^2}{1 + c^2}. \quad (10)$$

Proposition 2. *If $\mathcal{R}_0 < 1$ and $\sigma = 0$, then the zooplankton extinction equilibrium of system (9), \mathcal{E}_{np} , is locally asymptotically stable. If $\mathcal{R}_0 > 1$, it is unstable.*

Proof. See appendix A. □

From expression (10) it is apparent that the invasion number \mathcal{R}_0 may be interpreted as the average lifespan of zooplankton, a^{-1} , scaled down by a function of the phytoplankton carrying capacity, $c^2(1 + c^2)^{-1}$. Note that for fixed a , $\lim_{c \rightarrow \infty} \mathcal{R}_0 = a^{-1}$ and $\lim_{c \rightarrow 0} \mathcal{R}_0 = 0$. Similarly, for fixed c , $\lim_{a \rightarrow 0} \mathcal{R}_0 = \infty$ and $\lim_{a \rightarrow 1} \mathcal{R}_0 = c^2(1 + c^2)^{-1} <$

1. This, together with Prop. 2, indicates that when $\sigma = 0$, phytoplankton carrying capacity increases or the zooplankton loss rate decreases, the probability of zooplankton extinction will approach zero. When phytoplankton carrying capacity is low or the zooplankton loss rate is high, zooplankton extinction is more likely.

Proposition 3. *If $\sigma = 0$, then the system (9) has a unique coexistence equilibrium if and only if $\mathcal{R}_0 > 1$.*

Proof. Suppose that for the system (9), we have $\sigma = 0$,

$$\frac{dp}{d\tau} = \frac{dz}{d\tau} = \frac{dn}{d\tau} = 0,$$

and that $n, p, z > 0$. Then, the system has the following potential unique coexistence equilibrium:

$$\mathcal{E}_* = \begin{cases} p_* = \sqrt{\frac{a}{1-a}} \\ n_* = (2cs)^{-1} \left[n_b + \sqrt{n_b^2 + 4c^2 \tilde{k} \theta s^2} \right] \\ z_* = \frac{n_*}{p_*(\tilde{k} + n_*)} \left(1 - \frac{p_*}{c} \right) (1 + p_*^2) \end{cases} \quad (11)$$

where

$$n_b = -\tilde{k}s + c\theta s - cp_*\gamma + p_*^2\gamma.$$

Note that $\mathcal{R}_0 > 1$ if and only if $p_* < c$:

$$\begin{aligned} \mathcal{R}_0 = \frac{c^2}{a(1+c^2)} > 1 &\Leftrightarrow \frac{c^2}{1+c^2} > a \\ &\Leftrightarrow p_* = \sqrt{\frac{a}{1-a}} < \sqrt{\frac{c^2(1+c^2)^{-1}}{1-c^2(1+c^2)^{-1}}} = \sqrt{c^2} = c. \end{aligned}$$

Additionally, from its form, it is clear that $n_* > 0$. Thus, we may conclude that this expression for the coexistence equilibrium is biologically feasible. \square

Let

$$\begin{cases} \psi_1 = \frac{n_*}{\tilde{k} + n_*} \left(1 - \frac{p_*}{c} \right), \psi_2 = 2p_* \frac{p_*^2}{1 + p_*^2} z_*, \psi_3 = 2 \frac{p_*}{(1 + p_*^2)^2} z_*, \\ \psi_4 = \frac{n_*}{\tilde{k} + n_*} \cdot \frac{p_*}{c}, \psi_5 = \frac{p_*(c - p_*)}{c(\tilde{k} + n_*)} \left(1 - \frac{n_*}{\tilde{k} + n_*} \right), \xi_0 = a\tilde{\gamma}\psi_3(s + \gamma\psi_5), \\ \xi_1 = s(-\psi_1 + \psi_3 + \psi_4) + \gamma\psi_3\psi_5 + a\tilde{\gamma}\psi_3, \xi_2 = -\psi_1 + \psi_3 + \psi_4 + \psi_5 + s \\ \hat{\xi}_1 = \xi_1 + s\psi_1, \hat{\xi}_2 = \xi_2 + \psi_1, \mathcal{C}_1^1 = \frac{\psi_1 + a\tilde{\gamma}}{\psi_3 + \psi_4 + s\psi_5 + a\tilde{\gamma}}, \\ \mathcal{C}_1^2 = \frac{\xi_0 + \psi_1(\hat{\xi}_1 + s\hat{\xi}_2)}{\hat{\xi}_1\hat{\xi}_2 + s\psi_1^2}, \mathcal{C}_1 = \max\{\mathcal{C}_1^1, \mathcal{C}_1^2\} \end{cases} \quad (12)$$

where p_*, n_*, z_* are as defined in (11).

Proposition 4. *If $\mathcal{R}_0 > 1$ and $\sigma = 0$, then the coexistence equilibrium, \mathcal{E}_* (11), is locally asymptotically stable if*

$$\mathcal{C}_1 := \max\{\mathcal{C}_1^1, \mathcal{C}_1^2\} < 1 \quad (13)$$

and has a simple Hopf bifurcation in a parameter of interest, α , at value α_0 if

$$\mathcal{C}_1^1 < \mathcal{C}_1^2 = 1 \quad (14)$$

and

$$-\xi'_0(\alpha_0) + \xi_2(\alpha_0)\xi'_1(\alpha_0) + \xi_1(\alpha_0)\xi'_2(\alpha_0) \neq 0 \quad (15)$$

Proof. See appendix A. □

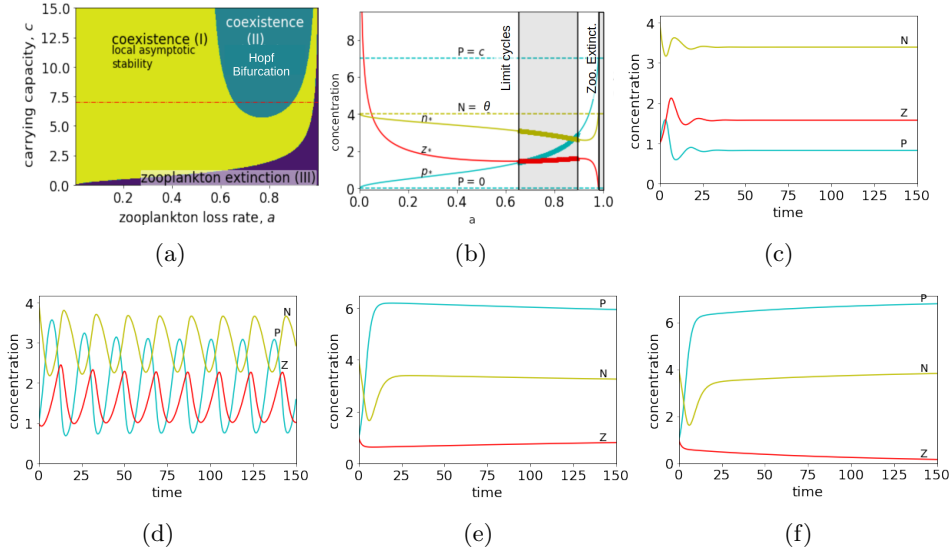


Fig. 3: Bifurcation diagrams and representative simulations for the NPZ system with linear zooplankton mortality. Blue, red, and yellow curves represent phytoplankton, zooplankton, and nutrients respectively. (a) Two-dimensional bifurcation diagram with respect to the model parameters a, c , representing the zooplankton mortality rate and the phytoplankton carrying capacity, respectively. (b) One-dimensional bifurcation diagram with respect to the parameter a when $c = 7$ (dashed red line in (a)). All other model parameters are as specified in table 2. (c-f) Time-dependent solutions demonstrating the qualitative dynamics when $c = 7$. The transitions are region 1 ($a = 0.4$) \rightarrow region 2 ($a = 0.7$) \rightarrow region 1 ($a = 0.98$) \rightarrow region 3 ($a = 0.999$).

We choose the notation \mathcal{C}_1 because, as shown in Prop. 3 (similarly with \mathcal{C}_2 in Prop. 8), it describes the qualitative nature of coexistence in the model with linear zooplankton loss term. While the above expressions (derived from the characteristic polynomial of the Jacobian with MatLab Symbolic Math Toolbox) do not have an easily interpreted biological meaning they are useful in two ways. First, they provide mathematically rigorous bounds for both local asymptotic stability and Hopf bifurcation of the coexistence equilibrium. Second, these expressions give an indication of which parameters are important to the qualitative dynamics of the model. Via these expressions, we can see that, in the case of linear zooplankton loss, the only parameters which affect the unique coexistence equilibrium and its asymptotic dynamics are a , zooplankton loss rate, and c , phytoplankton carrying capacity.

Hopf bifurcation is defined as the birth of a limit cycle from an equilibrium where the equilibrium changes stability via a pair of purely imaginary eigenvalues. The bifurcation can be supercritical or subcritical, resulting in stable or unstable limit cycles [32]. In model (9) with $\sigma = 0$ in the parameter region where Hopf bifurcation occurs we observe that these bifurcations occur around the values of bifurcation parameter a where $p_* \approx z_*$, and act as a transitory state from high to low phytoplankton abundance (see figure 3(b)).

3.2 Linear zooplankton loss term: a special case

Suppose that nutrient loss/exchange rate $s = 0$, $\tilde{\gamma} = \gamma$, and upon death, zooplankton instantaneously become nutrients. Then, system (9) is closed (ie. $\forall \tau \geq 0$, $n(\tau) + p(\tau) + z(\tau) = N_T = p(0) + z(0) + n(0)$). In this case, we may rewrite the system as:

$$\begin{cases} \frac{dp}{d\tau} = \frac{N_T - (p+z)}{\tilde{k} + N_T - (p+z)} p \left(1 - \frac{p}{c}\right) - \frac{p^2}{1+p^2} z \\ \frac{dz}{d\tau} = \gamma \left(\frac{p^2}{1+p^2} - a\right) z \\ \frac{dn}{d\tau} = -\frac{N_T - (p+z)}{\tilde{k} + N_T - (p+z)} p \left(1 - \frac{p}{c}\right) + (1-\gamma) \frac{p^2}{1+p^2} z + \gamma a z. \end{cases} \quad (16)$$

For this system, there are the following boundary equilibria: $\mathcal{E}_0 = (0, 0, N_T)^T$, $\mathcal{E}_{N_T} = (N_T, 0, 0)^T$, and $\mathcal{E}_c = (c, 0, N_T - c)^T$ (exists if and only if $N_T \geq c$). Also, note that for this version of the model, the $p = 0$ and $z = 0$ planes are invariant and if $n = 0$ (that is, $N_T = p + z$), then

$$\frac{dn}{d\tau} = (1-\gamma) \frac{p^2}{1+p^2} z + \gamma a z \geq 0. \quad (17)$$

Hence, the set $B = \{(p, z, n) : 0 \leq p+z \leq N_T\}$ is invariant (and indeed $p+z > N_T \Rightarrow n < 0$). Thus, we need only consider solutions on this set. Additionally, because we

may write $n(\tau) = N_T - p(\tau) - z(\tau)$, we need only consider the reduced system

$$\begin{cases} \frac{dp}{d\tau} = \frac{N_T - (p+z)}{k + N_T - (p+z)} p \left(1 - \frac{p}{c}\right) - \frac{p^2}{1+p^2} z = f_1(p, z) \\ \frac{dz}{d\tau} = \gamma \left(\frac{p^2}{1+p^2} - a\right) z = f_2(p, z) \end{cases} \quad (18)$$

Now, define the zooplankton invasion number:

$$\mathcal{R}_1 := \frac{1}{a} \cdot \frac{N_T^2}{1 + N_T^2} \quad (19)$$

Proposition 5. *If $N_T < c$ and $\mathcal{R}_1 < 1$, then the zooplankton extinction equilibrium \mathcal{E}_{N_T} is globally asymptotically stable in $B \setminus \{p = 0\}$. If $N_T > c$ or $\mathcal{R}_1 > 1$, it is unstable.*

Proof. First, note that the lines $p = 0$ and $z = 0$ are invariant. Then observe that the Jacobian of system (18) evaluated at \mathcal{E}_{N_T} is

$$J(\mathcal{E}_{N_T}) = \begin{pmatrix} \frac{-N_T(c-N_T)}{ck} & * \\ 0 & \gamma a(\mathcal{R}_1 - 1) \end{pmatrix}, \quad (20)$$

from this it is clear that if $N_T < c$ and $\mathcal{R}_1 < 1$, then \mathcal{E}_{N_T} is locally stable, and is unstable if either $N_T > c$ or $\mathcal{R}_1 > 1$.

Now observe that for this version of the model, the community collapse equilibrium \mathcal{E}_0 is always unstable since

$$J(\mathcal{E}_0) = \begin{pmatrix} \frac{N_T}{k+N_T} & 0 \\ 0 & -a\gamma \end{pmatrix}. \quad (21)$$

Note that

$$\begin{aligned} \mathcal{R}_1 = \frac{N_T^2}{a(1+N_T^2)} < 1 &\Leftrightarrow \frac{N_T^2}{1+N_T^2} < a \\ &\Leftrightarrow p_* = \sqrt{\frac{a}{1-a}} > \sqrt{\frac{N_T^2(1+N_T^2)^{-1}}{1-N_T^2(1+N_T^2)^{-1}}} = \sqrt{N_T^2} = N_T, \end{aligned} \quad (22)$$

where p_* is the p component of any possible coexistence equilibrium. Thus, when $N_T < c$ and $\mathcal{R}_1 < 1$, there are only two equilibria in B : \mathcal{E}_0 and \mathcal{E}_{N_T} . Since the model is closed, all of our solutions are bounded for $\tau \geq 0$. Thus, any solution contains $[0, \infty)$ in its domain and has a compact and non-empty ω -limit set.

Note that for $\phi = 1/p^2$, $N_T < c$, and $\mathcal{R}_1 < 1$, for any solution to (16) $(p, z)^T \in B \setminus (\{p = 0\} \cup \{z = 0\})$:

$$\begin{aligned} \frac{\partial}{\partial p} \left[\phi \frac{dp}{d\tau} \right] &= -\frac{1-p/c}{p} \left(\frac{\tilde{k}}{(\tilde{k} + N_T - (p+z))^2} \right) - \frac{N_T - (p+z)}{\tilde{k} + N_T - (p+z)} \cdot \frac{1}{p^2} \\ &\quad - \frac{2p}{(1+p^2)^2} z < 0 \\ \frac{\partial}{\partial z} \left[\phi \frac{dz}{d\tau} \right] &= \gamma \left(\frac{p^2}{1+p^2} - a \right) \frac{1}{p^2} \leq \frac{\gamma a}{p^2} (\mathcal{R}_1 - 1) < 0 \end{aligned} \quad (23)$$

since $\frac{p^2}{1+p^2}$ is an increasing function of p . Hence, when $N_T < c$ and $\mathcal{R}_1 < 1$,

$$\nabla \cdot (\phi(p) f(p, z)) = \frac{\partial}{\partial p} \left[\phi \frac{dp}{d\tau} \right] + \frac{\partial}{\partial z} \left[\phi \frac{dz}{d\tau} \right] < 0 \quad \forall (p, z)^T \in B \setminus (\{p = 0\} \cup \{z = 0\}). \quad (24)$$

Thus, by Dulac's criterion, it follows that there are no closed orbits wholly contained in $B \setminus (\{p = 0\} \cup \{z = 0\})$.

Now, notice that in the invariant line $N_T = n + p$ (ie. $z = 0$), $\frac{dz}{d\tau} = 0$ and if $p > 0$, then $\frac{dp}{d\tau} > 0$ when $p < N_T < c$. Similarly, on the invariant line $N_T = n + z$ ($p = 0$), \mathcal{E}_0 attracts all solutions. Let L stand for the ω -limit set of some point $(p_0, z_0, n_0)^T \in B \setminus (\{p = 0\} \cup \{z = 0\})$. Recall that there are two equilibria, \mathcal{E}_0 and \mathcal{E}_{N_T} , in B . Because \mathcal{E}_0 is a hyperbolic saddle-node it cannot belong to any heteroclinic cycle or homoclinic loop. Consequently, there are no heteroclinic cycles or homoclinic loops at all (Poincaré–Bendixson theorem). Hence, $L = \{\mathcal{E}_{N_T}\}$. It follows that \mathcal{E}_{N_T} is globally asymptotically stable in $B \setminus \{p = 0\}$. \square

Proposition 6. *The zooplankton extinction equilibrium $\mathcal{E}_c = (c, 0, N_T - c)^T$ exists if and only if $N_T \geq c$. Further, if $\mathcal{R}_0 < 1$ and $N_T > c$, then it is locally asymptotically stable. If $\mathcal{R}_0 > 1$, it is unstable.*

Proof. See appendix A. \square

3.3 Quadratic zooplankton loss ($\sigma = 1$)

Suppose that $n, p, z > 0$ and

$$\frac{dp}{d\tau} = \frac{dz}{d\tau} = \frac{dn}{d\tau} = 0.$$

It follows that in the case of quadratic zooplankton loss, any possible coexistence equilibrium must satisfy

$$\begin{cases} p_* = \sqrt{\frac{az_*}{1-az_*}}, \\ n_* = s^{-1}(s\theta - \gamma az_*^2), \\ 0 = az_*^2 + z_* + \frac{n_*}{k+n_*}p_* \left(1 - \frac{p_*}{c}\right), \end{cases} \quad (25)$$

which cannot be solved explicitly. Because of this, we now make use of the following result from general persistence theory:

Theorem (Existence of coexistence equilibrium, [33]) Suppose that

1. X is a closed, convex subset of a Banach Space,
2. ϕ has a compact attractor, B , of bounded subsets in X ,
3. ρ is continuous and concave,
4. ϕ is uniformly weakly persistent,
5. $\phi(t, \cdot)$ is compact for some $t > 0$.

Then, there exists an equilibrium x^* with $\rho(x^*) > 0$.

Proposition 7. *There exists at least one coexistence equilibrium in the system (9) when $\sigma = 1$.*

Proof. We first show that the system (9) is dissipative. Note that the planes where $p = 0$ and $z = 0$ are invariant, and when $n = 0$, $\frac{dn}{d\tau} > 0$. Then, define

$$A_p = \{(p, z, n)^T : p \geq c, z > 0, n > 0\} \quad (26)$$

and note that $\forall (p, z, n)^T \in A_p$, $\frac{dp}{d\tau} < 0$. Now define

$$\begin{aligned} A_z^{(2)} &= \{(p, z, n)^T : 0 < p \leq c, z > \mathcal{R}_0, n > 0\} \\ A_n &= \{(p, z, n)^T : 0 < p \leq c, 0 < z \leq \mathcal{R}_0, n > \hat{n}\} \end{aligned} \quad (27)$$

where $\hat{n} = s^{-1}((1 - \gamma)a\mathcal{R}_0^2 + s\theta)$. First, note that $\forall (p, z, n)^T \in A_z^{(2)}$

$$\frac{dz}{d\tau} \leq \tilde{\gamma}a(\mathcal{R}_0 - z)z < 0. \quad (28)$$

Next, observe that $\forall (p, z, n)^T \in A_n$,

$$\begin{aligned} \frac{dn}{d\tau} &\leq (1 - \gamma)\frac{c^2}{1 + c^2}\mathcal{R}_0 + s(\theta - n) \\ &= (1 - \gamma)a\mathcal{R}_0^2 + s(\theta - n) \\ &< 0. \end{aligned} \quad (29)$$

Hence $\forall(p, z, n)^T$ such that $p_0, z_0, n_0 \geq 0$,

$$\lim_{\tau \rightarrow \infty} (p(\tau), z(\tau), n(\tau))^T \in B = \{(p, z, n) : 0 \leq p \leq c, 0 \leq z \leq \mathcal{R}_0, 0 \leq n \leq \hat{n}\}.$$

Thus, system (9) is dissipative.

Note that when $\sigma = 1$, the Jacobian evaluated at equilibrium \mathcal{E}_{np} takes the form

$$J(\mathcal{E}_{np}) = \begin{pmatrix} A & 0 \\ * & -s \end{pmatrix}, \quad (30)$$

where

$$A = \begin{pmatrix} -\frac{\theta}{k+\theta} & -a\mathcal{R}_0 \\ 0 & \tilde{\gamma}a\mathcal{R}_0 \end{pmatrix}.$$

Thus if $\sigma = 1$, \mathcal{E}_{np} is always a hyperbolic saddle node.

Next we show that the system is robustly uniformly ρ -persistent, where $\rho = \min\{n(\tau), p(\tau), z(\tau)\}$.

We may consider the equilibria of the system as trivial periodic solutions. Applying corollary 4.7 of [34], we see, via proposition 4.1 and theorem 3.2 of [34], that phytoplankton are robustly persistent if the eigenvalue in the p direction of $J(\mathcal{E}_n)$, $\lambda_p^{\mathcal{E}_n} > 0$. Similarly, since zooplankton depend upon phytoplankton as a resource, we need only show the eigenvalue in the z direction of $J(\mathcal{E}_{np})$, $\lambda_z^{\mathcal{E}_{np}} > 0$ provided the first condition holds. Note that

$$J(\mathcal{E}_n) = \begin{pmatrix} \frac{\theta}{k+\theta} & 0 & 0 \\ 0 & -\tilde{\gamma}a(1-\sigma) & 0 \\ -\frac{\theta}{k+\theta} & 0 & -s \end{pmatrix}.$$

From this it is clear that $\lambda_p^{\mathcal{E}_n} = \theta(\tilde{k}+\theta)^{-1} > 0$. Next, notice that boundary equilibrium \mathcal{E}_{np} has $\lambda_z^{\mathcal{E}_{np}} = \eta\gamma\beta^{-1}a(\mathcal{R}_0 - (1-\sigma))$. From this, it is clear that this eigenvalue is strictly positive if $\sigma = 1$ or $\mathcal{R}_0 > 1$ and $\sigma = 0$.

Hence, all of the conditions for the existence of a coexistence equilibrium are either met or exceeded. \square

For arbitrary coexistence equilibrium $\mathcal{E}_* = (p_*, z_* n_*)^T$ satisfying (25), let

$$\left\{ \begin{array}{l} \nu_0 = a\tilde{\gamma}z_* [(\psi_3 + \psi_4)(\psi_5 + s) + \psi_5(\psi_1 + \psi_2(1 - \gamma)) + \psi_2\psi_5\gamma z_* + \psi_3sz_*] \\ \quad - a\tilde{\gamma}z_* [(\psi_1 + \psi_2)(\psi_5 + s) + \psi_5(\psi_3(1 - \gamma) + \psi_4) + \psi_3\psi_5\gamma z_* + \psi_2sz_*] \\ \nu_1 = (\psi_3 + \psi_4)(a\tilde{\gamma}z_* + \psi_5 + s) + a\tilde{\gamma}z_*(\psi_5 + s) + \psi_1\psi_5 + \psi_2\psi_5(1 - \gamma) \\ \quad - ((\psi_1 + \psi_2)(a\tilde{\gamma}z_* + \psi_5 + s) + a\tilde{\gamma}z_*^2\psi_2 + \psi_3(1 - \gamma) + \psi_4) \\ \nu_2 = \psi_3 + \psi_4 + a\tilde{\gamma}z_* + s - (\psi_1 + \psi_2) \\ \hat{\nu}_0 = \nu_0 + a\tilde{\gamma}z_* [(\psi_1 + \psi_2)(\psi_5 + s) + \psi_5(\psi_3(1 - \gamma) + \psi_4) + \psi_3\psi_5\gamma z_* + \psi_2sz_*], \\ \hat{\nu}_1 = \nu_1 + ((\psi_1 + \psi_2)(a\tilde{\gamma}z_* + \psi_5 + s) + a\tilde{\gamma}z_*^2\psi_2 + \psi_3(1 - \gamma) + \psi_4), \\ \hat{\nu}_2 = \nu_2 + \psi_1 + \psi_2, \mathcal{C}_2^1 = \frac{\hat{\nu}_2 - \nu_2}{\hat{\nu}_2}, \mathcal{C}_2^2 = \frac{\hat{\nu}_0 + \hat{\nu}_1(\hat{\nu}_2 - \nu_2) + \hat{\nu}_2(\hat{\nu}_1 - \nu_1)}{\hat{\nu}_1\hat{\nu}_2 + (\hat{\nu}_1 - \nu_1)(\hat{\nu}_2 - \nu_2) + (\hat{\nu}_0 - \nu_0)}, \\ \mathcal{C}_2^3 = \frac{\hat{\nu}_0 - \nu_0}{\hat{\nu}_0}, \mathcal{C}_2 = \max\{\mathcal{C}_2^1, \mathcal{C}_2^2, \mathcal{C}_2^3\}, \end{array} \right. \quad (31)$$

where ψ_i are as defined in system (12) and expressions were again derived from the characteristic polynomial of the Jacobian with MatLab Symbolic Math Toolbox.

Proposition 8. \mathcal{E}_* is locally asymptotically stable if

$$\mathcal{C}_2 < 1 \quad (32)$$

and has a simple Hopf bifurcation in a parameter of interest, α at point α_0 , if

$$\mathcal{C}_2^1 < \mathcal{C}_2^2 = 1 \quad (33)$$

and

$$-\nu'_0(\alpha_0) + \nu_2(\alpha_0)\nu'_1(\alpha_0) + \nu_1(\alpha_0)\nu'_2(\alpha_0) \neq 0 \quad (34)$$

Proof. See appendix A. □

As with Prop. 4, while it is difficult to directly interpret these quantities biologically, they indicate that many more parameters can affect the qualitative dynamics of the model.

In the case of a quadratic zooplankton loss term, studying these equations indicates a much broader subset of the model parameters can affect both the number of coexistence equilibria and the asymptotic dynamics of each such equilibrium. Specifically from the numerical generation of bifurcation diagrams (see GitHub [35]), we can see that the parameters which can affect both stability and number of equilibria are again a and c as well as the nutrient loss/exchange rate, s ; the intrinsic nutrient level, θ ; the zooplankton assimilation rate, γ ; and the nutrient update half saturation constant, \tilde{k} . In addition $\tilde{\gamma}$, which γ scaled by the ratio of maximum zooplankton grazing rate, η , to the phytoplankton response to light, β , can affect the asymptotic behavior of the system.

Table 1: Summary of threshold analysis from Sec. 3

Equilibrium $(p, z, n)^T$	Description
$\mathcal{E}_{np} = (c, 0, \theta)^T$	Boundary (zooplankton extinction), LAS if $\mathcal{R}_0 < 1$ and $\sigma = 0$ unstable otherwise (Props. 2, 7)
$\mathcal{E}_n = (0, 0, \theta)^T$	Boundary (community collapse), unstable (Prop. 1)
$\mathcal{E}_{N_T} = (N_T, 0, 0)^T$	Special case, boundary (zooplankton extinction) GAS if $\mathcal{R}_1 < 1$ and $N_T < c$ (Prop. 5).
$\mathcal{E}_c = (c, 0, N_T - c)^T$	Special case, boundary (zooplankton extinction) exists and LAS if $\mathcal{R}_0 < 1$ and $N_T > c$. (Prop. 6).
$\mathcal{E}_* = (p_*, z_*, n_*)^T$	<p>Coexistence ($\sigma = 0$): Unique existence iff $\mathcal{R}_0 > 1$ (Prop. 3) LAS if $\mathcal{C}_1 < 1$ (Prop. 4) Simple Hopf bifurcation if $\mathcal{C}_1^1 < \mathcal{C}_1^2 = 1$, condition (15) is satisfied (Prop. 4)</p> <p>Coexistence ($\sigma = 1$): Exists at least one (Prop. 7) For arbitrary coexistence equilibrium: LAS if $\mathcal{C}_2 < 1$ (Prop. 8) Simple Hopf bifurcation if $\mathcal{C}_2^1 < \mathcal{C}_2^2 = 1$, condition (33) is satisfied (Prop. 8)</p>

4 Extending threshold analysis to the NPZD Model and ecological implications

Here, we investigate the analytical and numerical properties of the full NPZD system (8) along with ecological implications of phytoplankton overpopulation during HABs and the effects of ecological disturbances on these dynamics.

Define phytoplankton persistence number

$$\mathcal{P}_0^p := \frac{1}{\tilde{\epsilon}} \cdot \frac{\theta}{k + \theta} \quad (35)$$

Proposition 9. *If $\mathcal{P}_0^p > 1$ then for the model (8) the phytoplankton population is robustly uniformly ρ -persistent where $\rho = \min_{\tau} p(\tau)$.*

Proof. See appendix A. □

We see that for this model \mathcal{P}_0^p is the average lifespan of phytoplankton scaled by a ratio of the intrinsic nutrient level of the system, with persistence being assured if $\tilde{\epsilon} < \theta/(k + \theta)$. We particularly focus on its implications for the zooplankton extinction equilibrium as well as the conditions for zooplankton persistence and the existence of at least one coexistence equilibrium.

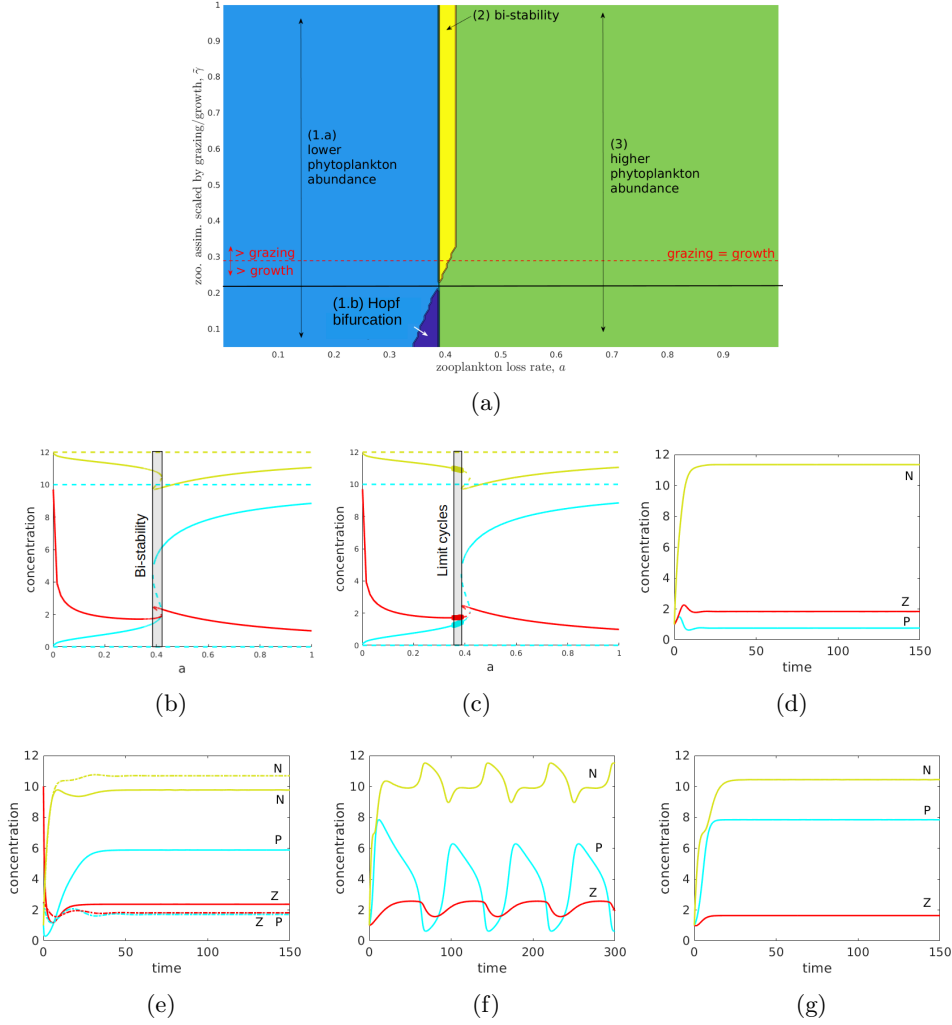


Fig. 4: Bifurcation diagrams for the NPZ subsystem with quadratic zooplankton mortality. Blue, red, and yellow curves represent phytoplankton, zooplankton, and nutrients respectively. **(a)** Two-dimensional bifurcation diagram with respect to the model parameters $\tilde{\gamma}$, and a . One-dimensional bifurcation diagrams in a , where the transitory state between low and high phytoplankton abundance is either **(b)** bi-stability with $\tilde{\gamma} = 0.29$, or **(c)** Hopf bifurcation with $\tilde{\gamma} = 0.1$. All other parameter values are given in table 2. **(d-g)** Time-dependent solutions of the qualitative model dynamics in different parameter regions. The transition from low to high phytoplankton abundance is either region 1a ($a = 0.3, \tilde{\gamma} = 0.29$) \rightarrow region 2 ($a = 0.41, \tilde{\gamma} = 0.29$) \rightarrow region 3 ($a = 0.6, \tilde{\gamma} = 0.29$) or region 1a \rightarrow region 1b ($a = 0.37, \tilde{\gamma} = 0.1$) \rightarrow region 3 dependent on the value of $\tilde{\gamma}$.

The model (8) has two boundary equilibria, zooplankton extinction equilibrium $\mathcal{E}_{npd} = (\hat{p}, 0, \theta, \hat{d})^T$, where

$$\begin{cases} \hat{p} = c \left(1 - \frac{1}{\mathcal{P}_0^p}\right) \\ \hat{d} = \frac{\tilde{\epsilon}c}{\psi} \left(1 - \frac{1}{\mathcal{P}_0^p}\right), \end{cases} \quad (36)$$

and community collapse equilibrium $\mathcal{E}'_n = (0, 0, \theta, 0)^T$. Now define the zooplankton invasion number

$$\mathcal{R}_0^z := \max\{\mathcal{R}_{0,1}^z, \mathcal{R}_{0,2}^z, \mathcal{R}_{0,3}^z, \mathcal{R}_{0,4}^z\}, \quad (37)$$

where

$$\begin{cases} b_1 = \tilde{\alpha}c(1 - 1/\mathcal{P}_0^p), b_2 = \frac{c\tilde{k}(\mathcal{P}_0^p - 1)}{(\mathcal{P}_0^p(\tilde{k} + \theta))^2}, b_3 = \frac{c(1 - 1/\mathcal{P}_0^p)}{\mathcal{P}_0^p(\tilde{k} + \theta)}(1 - \tilde{\epsilon}) + s \\ \mathcal{R}_{0,1}^z := \frac{c(1 - 1/\mathcal{P}_0^p)(\xi + c(1 - 1/\mathcal{P}_0^p))}{\tilde{\alpha}(1 + c^2(1 - 1/\mathcal{P}_0^p)^2)}, \mathcal{R}_{0,2}^z := \frac{\tilde{\epsilon}(\mathcal{P}_0^p - 1)}{b_3 + \psi} \\ \mathcal{R}_{0,3}^z := \frac{((b_3 + \psi)(b_2 + b_3 + \psi) + \tilde{\epsilon}(\tilde{\epsilon}b_2 + \psi b_3))(\mathcal{P}_0^p - 1)}{(b_3 + \psi)(\tilde{\epsilon}b_2 + \psi b_3) + \tilde{\epsilon}((\mathcal{P}_0^p - 1)(b_2 + b_3 + \psi) + \psi(b_2 + b_3))(\mathcal{P}_0^p - 1)} \\ \mathcal{R}_{0,4}^z := \frac{\mathcal{R}_{0,3}^z + \mathcal{R}_0^p}{\mathcal{R}_{0,3}^z \mathcal{R}_0^p + 1} \end{cases} \quad (38)$$

These expressions are complex and so difficult to interpret directly, though we observe that they are each functions of \mathcal{P}_0^p (as well as other model parameters).

Proposition 10. *For the model (8), boundary equilibrium \mathcal{E}_{npd} exists if and only if $\mathcal{P}_0^p > 1$. It is locally asymptotically stable if $\mathcal{R}_0^z < 1$, and is unstable if $\mathcal{R}_0^z > 1$.*

Proof. The existence of \mathcal{E}_{npd} if and only if $\mathcal{P}_0^p > 1$ is clear from its form. Note that the Jacobian of model (8) evaluated at \mathcal{E}_{npd} is

$$J(\mathcal{E}_{npd}) = \begin{pmatrix} \tilde{\epsilon}(\mathcal{P}_0^p - 1) & -\frac{\tilde{\alpha}c(1-1/\mathcal{P}_0^p)}{\xi+c(1-1/\mathcal{P}_0^p)}\mathcal{R}_{0,1}^z & \frac{c\tilde{k}(\mathcal{P}_0^p-1)}{(\mathcal{P}_0^p)^2(\tilde{k}+\theta)^2} & 0 \\ 0 & \tilde{\alpha}\tilde{\gamma}c(1-1/\mathcal{P}_0^p)(\mathcal{R}_{0,1}^z - 1) & 0 & 0 \\ \tilde{\epsilon}(\mathcal{P}_0^p - 2) & 0 & -\left(\frac{c(1-1/\mathcal{P}_0^p)}{\mathcal{P}_0^p(\tilde{k}+\theta)}(1-\tilde{\epsilon})+s\right) & \psi \\ \tilde{\epsilon} & (1-\gamma)\frac{\tilde{\alpha}c(1-1/\mathcal{P}_0^p)}{\xi+c(1-1/\mathcal{P}_0^p)}\mathcal{R}_{0,1}^z & 0 & -\psi \end{pmatrix}. \quad (39)$$

which has characteristic polynomial

$$\begin{aligned} \chi_{J(\mathcal{E}_{npd})}(\lambda) &= f(\lambda) \cdot g(\lambda) \\ &= (\lambda - b_1(\mathcal{R}_{0,1}^z - 1))[\lambda^3 + (b_3 + \psi - \tilde{\epsilon}(\mathcal{P}_0^p - 1))\lambda^2 \\ &\quad + (\tilde{\epsilon}(b_2 - (\mathcal{P}_0^p - 1)(b_2 + b_3 + \psi)) + \psi b_3)\lambda - \tilde{\epsilon}\psi(b_2 + b_3)(\mathcal{P}_0^p - 1)]. \end{aligned} \quad (40)$$

The positivity of b_1, b_2, b_3 is assured by $\mathcal{P}_0^p > 1$ and the form of \mathcal{P}_0^p . The sign of the eigenvalue $\lambda_1 = b_1(\mathcal{R}_{0,1}^z - 1)$ is clear. Thus we turn to Hurwitz determinants to

find conditions on the sign of the real parts of the roots of $g(\lambda)$:

$$\begin{aligned} H_1 &= b_3 + \psi - \tilde{\epsilon}(\mathcal{P}_0^p - 1) \\ H_2 &= H_1(\tilde{\epsilon}(b_2 - (\mathcal{P}_0^p - 1)(b_2 + b_3 + \psi)) + \psi b_3) + \tilde{\epsilon}\psi(b_2 + b_3)(\mathcal{P}_0^p - 1) \\ H_3 &= -\tilde{\epsilon}\psi(b_2 + b_3)(\mathcal{P}_0^p - 1)H_2 \end{aligned} \quad (41)$$

Next note that for Hurwitz determinant H_i , $1 \leq i \leq 3$, $H_i > 0$ if and only if $R_{0,i+1} < 1$. The desired result follows. \square

Now define zooplankton persistence number

$$\mathcal{P}_0^z := \min\{\mathcal{P}_0^p, \mathcal{R}_{0,1}^z\}, \quad (42)$$

where

$$\begin{aligned} \mathcal{R}_{0,1}^z &= \frac{c(1 - 1/\mathcal{P}_0^p)(\xi + c(1 - 1/\mathcal{P}_0^p))}{\tilde{\alpha}(1 + c^2(1 - 1/\mathcal{P}_0^p)^2)} \\ &= \frac{\hat{p}(\xi + \hat{p})}{\tilde{\alpha}(1 + \hat{p}^2)} \end{aligned} \quad (43)$$

Much like the quadratic zooplankton loss term case of model (9), an explicit expression for the coexistence equilibria of the extended model does not exist, however, any potential coexistence equilibrium must satisfy the following system of equations:

$$\begin{cases} n_* = \frac{1}{2s} \left(-n_b + \sqrt{n_b^2 + 4sk(\tilde{\epsilon}\gamma p_* + s\theta)} \right) \\ z_* = \frac{1 + p_*^2}{p_*} \left(\frac{n_*}{\tilde{k} + n_*} \left(1 - \frac{p_*}{c} \right) - \tilde{\epsilon} \right) \\ d_* = \frac{1}{\psi} \left((1 - \gamma) \frac{p_*}{1 + p_*^2} + \tilde{\epsilon} p_* \right) \\ 0 = \frac{p_*^2}{1 + p_*^2} - az_* - \frac{\tilde{\alpha} p_*}{\xi + p_*} \end{cases} \quad (44)$$

where

$$n_b = s(\tilde{k} - \theta) - \tilde{\epsilon}\gamma p_* + \gamma p_* \left(1 - \frac{p_*}{c} \right).$$

The positivity of n_* and d_* is clear from their forms provided $p_* > 0$. Therefore we need to provide a condition such that there exists at least one $p_* > 0$ for which the resulting $z_* > 0$, which as we show below is $\mathcal{P}_0^z > 1$.

Proposition 11. *For the model (8), if $\mathcal{P}_0^z > 1$, then zooplankton population is robustly uniformly ρ -persistent for $\rho = \min_{\tau} z(\tau)$ and there exists at least one coexistence equilibrium.*

Proof. See appendix A. \square

We make four key observations about the persistence numbers of zooplankton and phytoplankton which are relevant to our simulations.

$$\begin{cases} \lim_{\hat{p} \rightarrow c} \mathcal{P}_0^z = \lim_{\mathcal{P}_0^p \rightarrow \infty} \mathcal{P}_0^z = \frac{1}{\tilde{\alpha}} \\ \lim_{\theta \rightarrow \infty} \mathcal{P}_0^p = \frac{1}{\tilde{\epsilon}}, \quad \lim_{\theta \rightarrow 0} \mathcal{P}_0^p = 0 \end{cases} \quad (45)$$

and further that, for fixed \mathcal{P}_0^p ,

$$\begin{cases} \lim_{\tilde{\alpha} \rightarrow \infty} \mathcal{P}_0^z = \lim_{\xi \rightarrow 0} \mathcal{P}_0^z = 0 \\ \lim_{\tilde{\alpha} \rightarrow 0} \mathcal{P}_0^z = \lim_{\xi \rightarrow \infty} \mathcal{P}_0^z = \infty \end{cases} \quad (46)$$

The NPZD model also presents interesting complex bifurcation dynamics including forward hysteresis (see figure 5). In the context of population dynamics, forward hysteresis refers to the appearance of multiple local attractors when a threshold condition (usually a condition analogous to the basic reproduction number, \mathcal{R}_0 , in disease dynamical systems models) is larger than one [36]. For our model specifically, the curve of coexistence equilibria bifurcates from the zooplankton extinction equilibrium when $\mathcal{P}_0^z > 1$. In (a)-(c), we observe that the curve of phytoplankton equilibria in particular follows a pattern of hysteresis where the transitory state between high and low phytoplankton abundance is a region of bi-stability with model trajectory dependent on initial conditions. In this region of bi-stability, we note that the basin of attraction for the lower abundance equilibrium is in a neighborhood where the initial phytoplankton and zooplankton populations are approximately equal (see GitHub [35]) (d) sensitivity of \mathcal{P}_0^z to variation in ξ , $\tilde{\alpha}$. In Fig. 5(a), we observe that zooplankton will go (locally) extinct when the maximum harmful effect of phytoplankton is more than twice that of the maximum zooplankton grazing rate. In (b), we see that zooplankton will go (locally) extinct when the square root of the half-saturation constant for grazing is more than twice the half saturation of harmful effect (c) phytoplankton population decreases as a function of \mathcal{P}_0^z , reflecting the top-down regulation of phytoplankton population by zooplankton predation. For the model (8) Hopf bifurcation can also occur (see figure 6). Notice that, similarly to model (9) (see figure 4(b)), the region of stable limit cycles is a transitory state between low and high phytoplankton abundance when $\tilde{\gamma}$ is sufficiently small.

We observe that our model is capable of capturing a wide range of plankton population dynamics as a function of \mathcal{P}_0^z and \mathcal{P}_0^p . To quantify this we define what we term the balance of the ecosystem,

$$\mathcal{B} := 1 - \frac{\mathcal{P}_0^z}{\mathcal{P}_0^p}, \quad (47)$$

with the ideal balance being $\mathcal{B} = 0$ (see figures 5, 8), and so $\mathcal{P}_0^z = \mathcal{P}_0^p$, and having a positive (negative) value when phytoplankton (zooplankton) are favored. We observe in particular that our simulations suggest harmful algal blooms, which mathematically we define as a period of time where $dp/d\tau > 0$ and $dz/d\tau < 0$, occur from approximately when $\mathcal{B} > 0.5$ for our choice of other model parameters. This is chosen because

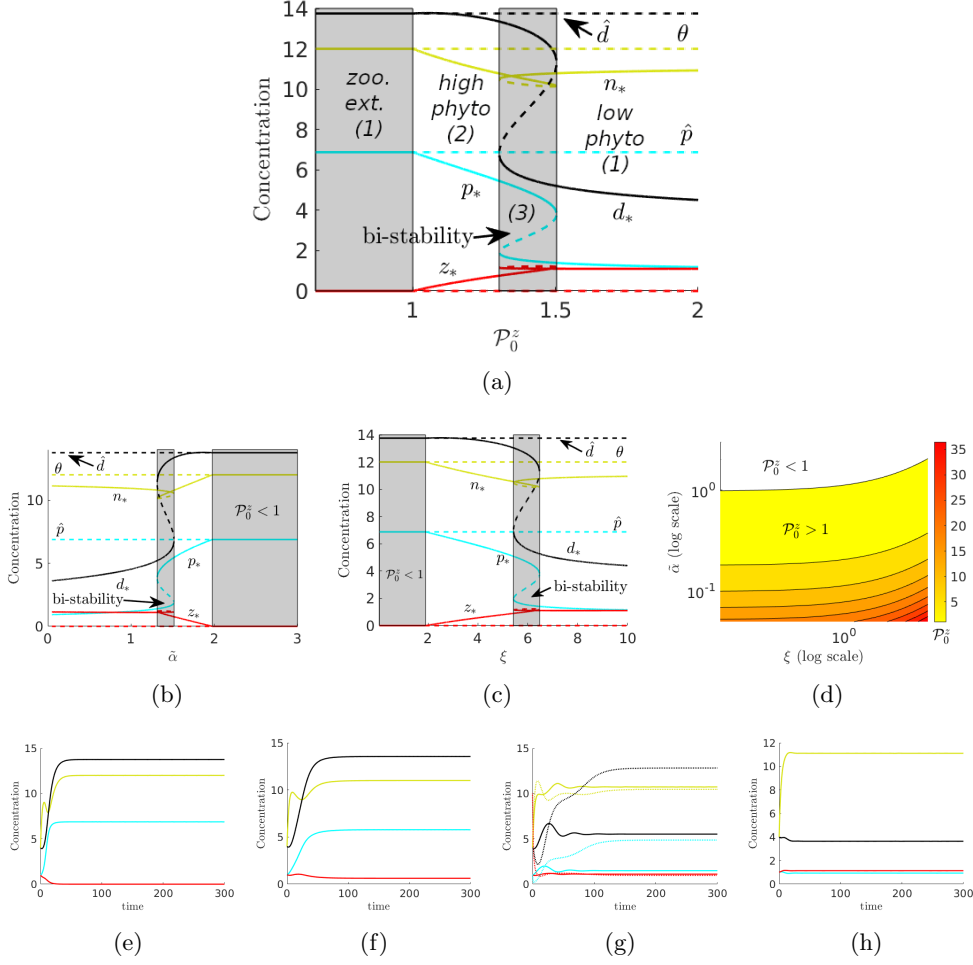


Fig. 5: Bifurcation diagrams for the rescaled model (9) with $\tilde{\gamma} = 0.29$ and $\mathcal{P}_0^p \approx 3.2$ during nutrient influx ($\theta = 12$) when $a = 0.4$. All other parameter values are in table 2. Blue, red, yellow, and black curves represent phytoplankton, zooplankton, nutrients, and detritus, respectively. In (a) we present the bifurcation diagram for different values of \mathcal{P}_0^z , which is a function of parameters $\tilde{\alpha}, \xi$. In (b) and (c) we present one-dimensional bifurcation diagrams in $\tilde{\alpha}$ with $\xi = 7$ and ξ with $\tilde{\alpha} = 1.25$ respectively. Observe that the Phytoplankton population decreases as a function of \mathcal{P}_0^z . In (d), sensitivity of \mathcal{P}_0^z to variation in $\xi, \tilde{\alpha}$ is displayed. (e)-(h) Time-dependent solutions demonstrating the qualitative dynamics in different parameter regions. The transition from high to low phytoplankton abundance is region 1 ($\mathcal{P}_0^z = 0.62 \Rightarrow \mathcal{B} = 0.81$) \rightarrow region 2 ($\mathcal{P}_0^z = 1.24 \Rightarrow \mathcal{B} = 0.61$) \rightarrow region 3 ($\mathcal{P}_0^z = 1.41 \Rightarrow \mathcal{B} = 0.56$) \rightarrow region 2 ($\mathcal{P}_0^z = 19.8 \Rightarrow \mathcal{B} = -5.2$).

it indicates that despite increasing abundance in the phytoplankton (prey) population, the zooplankton (predator) population still decreases. Moreover, zooplankton extinction occurs when \mathcal{B} approaches 1 (see figure 5(e)-(h) and supplementary figures C3-C5).

Thus - as the intrinsic nutrient level of the ecosystem increases in the scenario of a eutrophication event - \mathcal{P}_0^P will increase. And *if* we are in the region of the parameter space representing an unhealthy ecosystem, so will the size of the region where robust persistence of zooplankton is not assured. Similarly in the scenario of a re-oligotrophication event as the intrinsic nutrient level of the ecosystem decreases the balance of the ecosystem will change to (temporarily) favor zooplankton - reflecting the key biological reality we seek to capture with our model.

4.1 Incorporating seasonality and ecological disturbances

Eutrophication (re-oligotrophication) events may occur at different times, have different peak (trough) nutrient levels, and have different durations; thus here we incorporate seasonality. For a given event, consider the disturbance function, $\theta_d(\tau)$ where

$$\begin{cases} \theta_d(\tau) = \theta \pm \frac{M_\theta}{\max_\tau g(\omega, \tau)} g(\omega, \tau) \\ g(\tau) = \frac{1}{\omega^2} \tau e^{-\tau/\omega}, \end{cases} \quad (48)$$

with M_θ as the maximum intrinsic nutrient level increase/decrease relative to baseline level θ and ω , a scale parameter, which controls the duration of the disturbance. We note that this is a modified gamma distribution which is chosen for its flexibility in representing different disturbance curves. As we illustrate in Fig. 7, the duration of the disturbance increases with ω . Then we define

$$\theta(\tau) = \begin{cases} \theta & \tau < \tau_* \\ \theta_d(\tau) & \tau \geq \tau_* \end{cases} \quad (49)$$

where τ_* is the disturbance start time.

To incorporate seasonality of light availability we introduce the forcing term $f_s(\tau)$ into our re-scaled model (8):

$$\begin{cases} f_s(\tau) = 1 + \frac{1}{2} \sin\left(\frac{2\pi\tau}{100}\right) \\ \tilde{\gamma}_s(\tau) = \frac{\tilde{\gamma}}{f_s(\tau)}. \end{cases}, \quad (50)$$

which is the same seasonality function considered in [25] and [24] (chosen so that the mean value of f_s is one over a complete period).

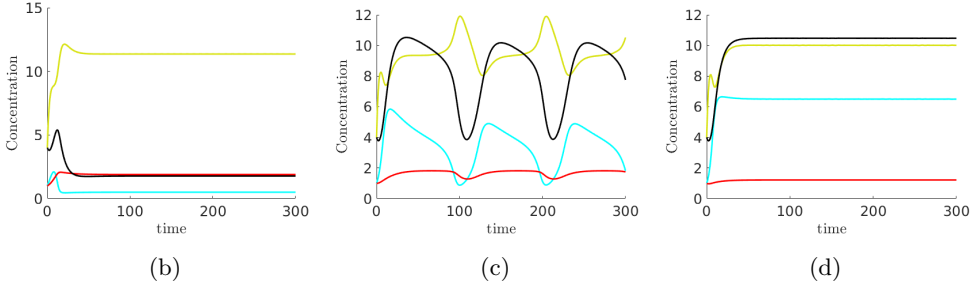
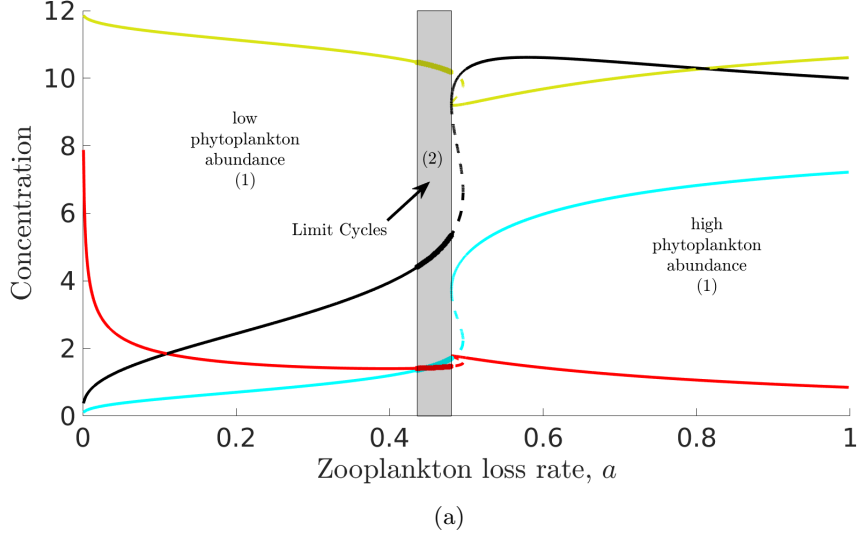


Fig. 6: One-dimensional bifurcation diagram of the model (8) in a under a parameter regime where the model displays Hopf bifurcation. Notice that, analogous to model (9) (see figure 4) the region of stable limit cycles is a transitory state between low and high phytoplankton abundance. Parameter values used are: $\tilde{k} = 0.5, c = 10, \tilde{\epsilon} = 0.15, \tilde{\gamma} = 0.1, \tilde{\alpha} = 0.5, \theta = 12, \psi = 0.15, \gamma = 0.5, \xi = 20$ ($\Rightarrow \mathcal{P}_0^p = 6.4, \mathcal{P}_0^z = 7.65, \mathcal{B} = -0.196$). (b)-(d) Time-dependent solutions demonstrating the qualitative dynamics in different parameter regions. The transition from low to high phytoplankton abundance is region 1 ($a = 0.1$) \rightarrow region 2 ($a = 0.47$) \rightarrow region 1 ($a = 0.7$).

Finally, putting everything together we arrive at the model,

$$\begin{cases} \frac{dp}{d\tau} = f_s(\tau) \frac{n}{\tilde{k} + n} p \left(1 - \frac{p}{c}\right) - \frac{p^2}{1 + p^2} z - \tilde{\epsilon} p \\ \frac{dz}{d\tau} = \tilde{\gamma}_s(\tau) \left[\frac{p^2}{1 + p^2} - \frac{\tilde{\alpha} p}{\xi + p} - az \right] z \\ \frac{dn}{d\tau} = -\frac{n}{\tilde{k} + n} p \left(1 - \frac{p}{c}\right) + s(\theta(\tau) - n) + \psi d \\ \frac{dd}{d\tau} = (1 - \gamma) \frac{p^2}{1 + p^2} z + \tilde{\epsilon} p - \psi d, \end{cases} \quad (51)$$

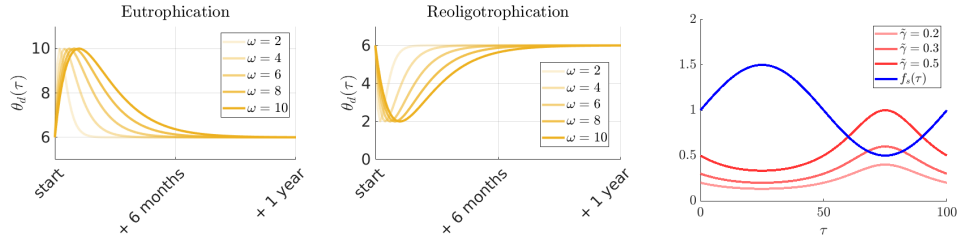


Fig. 7: Incorporating seasonal variation in light availability and ecological disturbances into the model. The duration of the disturbance increases with parameter ω for disturbance function $\theta_d(\tau, \omega)$ (**a-b**). Parameter M_θ dictates the peak nutrient level during a eutrophication event (**a**), and through nutrient level during a re-oligotrophication event (**b**). In (**c**) we display seasonality functions $f_s(\tau)$, and $\tilde{\gamma}_s(\tau)$ (with different values of model parameter $\tilde{\gamma}$).

A table with a detailed summary of all model terms for the system (51) is available in the appendices (see table B1).

Table 2: Descriptions of model parameters, values, and sources

Param.	Description	Value(s)	Source
\tilde{k}	Michaelis-Menton half saturation	0.5	[24, 25]
γ	zooplankton assimilation	0.5	[24, 25]
$\tilde{\gamma}$	zooplankton assimilation scaled by ratio of light response and grazing rates	0.29 (0,1)	[25] [24, 25]
c	Phytoplankton carrying capacity	10 (0,15)	[24, 25]
a	Zooplankton loss rate	(0,1)	[24, 25]
s	nutrient loss/exchange rate	0.3	[24, 25]
θ	Intrinsic nutrient level	4 12	[24, 25]
p_0	Initial phytoplankton	1 [0.375,10]	[24, 25]
z_0	Initial zooplankton	1 [0.1,10]	[24, 25]
n_0	Initial nutrients	4 1	[24, 25]
ψ	Detritus decay rate	0.15	based on [28]
$\bar{\epsilon}$	Phytoplankton natural mortality rate	0.3	assumed
$\bar{\alpha}$	Maximum harmful affect of phytoplankton	(0,3)	–
ξ	Half-saturation of harmful affect	(0,10)	–
M_θ	Peak/trough nutrient level during disturbance	[0, 12]	–
ω	Duration of disturbance	[2, 100]	–

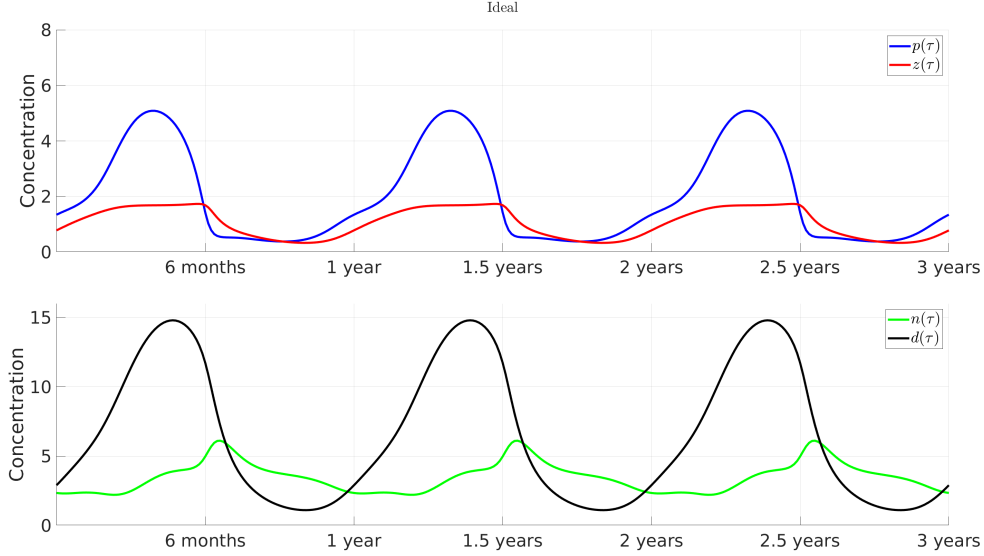


Fig. 8: An ideal healthy ecosystem prior to disturbance ($\mathcal{B} = 0$) with seasonality incorporated into the time simulations (model (51)). The top panel displays plankton populations and the bottom nutrient and detritus levels. $\tilde{k} = 0.5, c = 10, \tilde{\epsilon} = 0.3, \tilde{\gamma} = 0.29, \tilde{\alpha} = 0.85, \theta = 4, \psi = 0.15, \gamma = 0.5, \xi = 10, a = 0.4, s = 0.3$. (for the unforced model (8), $\mathcal{P}_0^p \approx \mathcal{P}_0^z \approx 3$).

4.2 Ecological implications

\mathcal{P}_0^z and \mathcal{P}_0^p as measures of ecosystem health

Eutrophication

We further observe that the further out of ideal balance an ecosystem is the more likely that zooplankton will be at risk of (local) extinction during a disturbance (see figure 9) - with an already unhealthy ecosystem which favors phytoplankton being more vulnerable to (additional) eutrophication. Thus, when ecological factors external to the particular eutrophication event have changed the composition of the existing phytoplankton assemblage there is an elevated risk of this and subsequent knock-on effects from total deregulation of phytoplankton populations with potential far-reaching up-trophic level consequences.

Reoligotrophication

In contrast to eutrophication, even a previously healthy ecosystem may be at risk of plankton community collapse provided a prolonged period of re-oligotrophication (see figure 10). Model simulations suggest that even a single year of nutrient depletion is sufficient to cause this collapse. This may explain the relatively rapid onset of such events in world rivers described by [11].

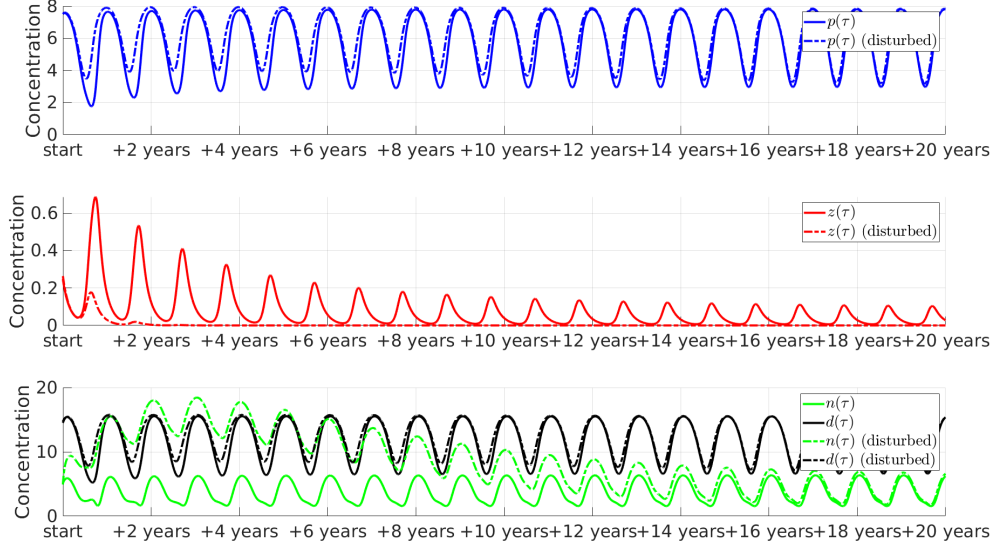


Fig. 9: Eutrophication event in an unhealthy ecosystem a priori favoring phytoplankton. Solid lines represent the undisturbed solution and dashed-and-dotted lines the disturbed solution. If the ecosystem balance, \mathcal{B} , sufficiently favors phytoplankton then an influx of nutrients can cause zooplankton extinction (middle panel). The parameter values used are $\tilde{k} = 0.5$, $c = 10$, $\tilde{c} = 0.3$, $\tilde{\gamma} = 0.29$, $\tilde{\alpha} = 2.81$, $\theta = 4$, $\psi = 0.15$, $\gamma = 0.5$, $\xi = 10$, $a = 0.4$, $s = 0.3$, $M_\theta = 12$, $\omega = 308$ (for the unforced model (8)), $\mathcal{P}_0^p \approx 3$, $\mathcal{P}_0^z \approx 0.9$, $\mathcal{B} \approx 0.71$).

5 Discussion

Starting from a base NPZ modeling framework, we incorporated the harmful effects of phytoplankton overpopulation on zooplankton during HABs, representing a crucial next step in HAB modeling [20], and split the nutrient compartment to formulate an NPZD model. We then mathematically analyze the NPZ system upon which this new model is based - deriving global stability conditions for the zooplankton extinction equilibrium in terms of zooplankton invasion number for a special case of the linear mortality model as well as local stability, Hopf bifurcation, and derived existence conditions for the coexistence equilibria of the NPZ model with both quadratic and linear zooplankton mortality. We provided one and two-parameter bifurcation diagrams for both models, showing forward hysteresis with bi-stable dynamics and Hopf bifurcation in the quadratic loss case depending on parameter values, and either Hopf bifurcation or transcritical bifurcation in the linear loss case. Finally, we extended the threshold analysis to the NPZD model, which displays both forward hysteresis with bi-stability and Hopf bifurcation, and examined ecological implications after incorporating seasonality and ecological disturbances in the form of eutrophication and re-oligotrophication events. Ultimately we quantified ecosystem health in terms of the relative values of

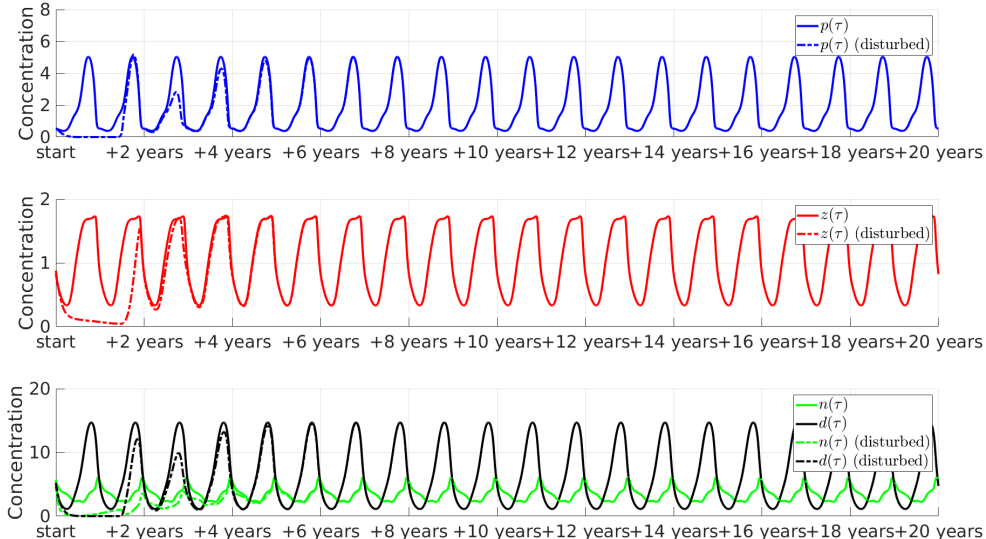


Fig. 10: Re-oligotrophication event in an a priori healthy ecosystem. Solid lines represent the undisturbed solution and dashed-and-dotted lines the disturbed solution. Mathematically, the plankton populations eventually recover to their pre-disturbance dynamics (top and middle panels). However, in reality, plankton populations may go extinct during the phase at which they are in low concentration, in this simulation approximately from one to three years post-disturbance. The parameter values used are: $\tilde{k} = 0.5, c = 10, \tilde{\epsilon} = 0.3, \tilde{\gamma} = 0.29, \tilde{\alpha} = 0.85, \theta = 4, \psi = 0.15, \gamma = 0.5, \xi = 10, a = 0.4, s = 0.3, M_\theta = 4, \omega = 100$ (for the unforced model (8), $\mathcal{P}_0^p \approx \mathcal{P}_0^z \approx 3$).

the robust persistence thresholds for phytoplankton and zooplankton and found (i) ecosystems sufficiently favoring phytoplankton, as measured by the relative values of plankton persistence numbers, are vulnerable to both HABs and (local) zooplankton extinction (ii) even balanced ecosystems are extremely sensitive to nutrient depletion over relatively short time-scales.

Modeling can provide crucial insights into functional understandings of population dynamics and interactions between ecosystem species and functional groups. Phytoplankton occupy niches in part based upon water temperature and nutrient composition [6–8]. Thus phytoplankton niche loss due to anthropologically driven rising water temperatures may cause increased competition in phytoplankton populations and shifts in phytoplankton assemblage composition. We found that the increasing frequency of harmful algal blooms may be explained, at least in part, by these shifting compositions of phytoplankton assemblages towards types of phytoplankton with more severe harmful effects due to overpopulation as the overall nutrient richness and temperature increase ([9]), represented by a decrease in \mathcal{P}_0^z and a shift in balance towards phytoplankton and that this may be exacerbated by eutrophication events, with already unhealthy ecosystems risking (local) zooplankton extinction provided

a eutrophication event of sufficient severity occurs (figure 9), representing a tipping point or critical transition [37–39].

In contrast to eutrophication, we found that even a previously healthy ecosystem is extremely vulnerable to prolonged re-oligotrophication. Model simulations suggest that only one year of nutrient depletion relative to typical intrinsic levels, could cause plankton population collapse. Importantly, original conditions were not recovered by simply reversing the course of nutrient flow showing clear evidence of a tipping point. This mirrors the perspective of [11] and may explain the relatively rapid onset of such events in comparison to eutrophication events (see figure 10).

Plankton, by definition, cannot swim against large-scale currents, and of course, live in many ecosystems which are affected by strong currents [1]. Thus, in many settings such as a river, the interplay between biological and physical dynamics is an important factor in the occurrence and severity of harmful algal blooms. However, a crucial step to understanding the population dynamics resulting from these complex interactions is to first understand bloom dynamics in a simpler physical setting, as we have here. The interplay between physical and biological factors is typically described via a one-way coupling to a diffusion-advection equation with a system of ODEs such as model (5) [27]. In this framework, the NPZD model can be thought of as the biological dynamics at physical location x and time t . Thus, future work should incorporate fluid dynamics into our modeling framework to understand the interplay between physical and biological factors in the context of ecological disturbances and HABs. Finally, given the potential utility of \mathcal{P}_0^p and particularly \mathcal{P}_0^z as ecosystem monitoring tools - our model should be parameterized to specific ecosystems and specific eutrophication and re-oligotrophication events.

Acknowledgments

The authors would like to thank Zachary Topor for informative discussions of plankton ecology. J.C.M is supported by a Zuckerman Foundation STEM leadership postdoctoral scholarship. During the main portion of this work, J.C.M. and H.G. were partially supported by a U.S. NSF RAPID grant (no. DMS-2028728) and NSF grant (no. DMS-1951759), and H.G. by a grant from the Simons Foundation/SFARI 638193.

Data availability statement

All software for this project is available under a CC-BY-NC 4.0 license and is archived in the Zenodo repository <https://doi.org/10.5281/zenodo.7650341> in citeable format.

Appendix

A. Proofs not appearing in the main text

Proof. (Prop. 1) Consider the Jacobian matrix evaluated at this point, which is

$$J(\mathcal{E}_n) = \begin{pmatrix} \frac{\theta}{k+\theta} & 0 & 0 \\ 0 & -\tilde{\gamma}a(1-\sigma) & 0 \\ -\frac{\theta}{k+\theta} & 0 & -s \end{pmatrix}. \quad (52)$$

From the form of (52) it is readily apparent that \mathcal{E}_n is always unstable. \square

Proof. (Prop. 2) Note that when $\sigma = 0$, the Jacobian evaluated at equilibrium \mathcal{E}_{np} takes the form of

$$J(\mathcal{E}_{np}) = \begin{pmatrix} A & 0 \\ * & -s \end{pmatrix}, \quad (53)$$

where

$$A = \begin{pmatrix} -\frac{\theta}{k+\theta} & -a\mathcal{R}_0 \\ 0 & \tilde{\gamma}a(\mathcal{R}_0 - 1) \end{pmatrix}. \quad \square$$

Proof. (Prop. 4) First, note that given system (8) and $\sigma = 0$ the Jacobian matrix evaluated at \mathcal{E}_* is,

$$J(\mathcal{E}_*) = \begin{pmatrix} \psi_1 + \psi_2 - \psi_3 - \psi_4 & -a & \psi_5 \\ \tilde{\gamma}z_*(\psi_3 - \psi_2) & 0 & 0 \\ -\psi_1 + (1-\gamma)(\psi_3 - \psi_2) + \psi_4 & a(1-\gamma) & -(\psi_5 + s) \end{pmatrix} \quad (54)$$

It follows that we have characteristic polynomial (assisted by MatLab Symbolic Math Toolbox):

$$\chi_{J(\mathcal{E}_*)}(\lambda) = \lambda^3 + \xi_2\lambda^2 + \xi_1\lambda + \xi_0. \quad (55)$$

Thus we have Hurwitz determinants, H_i :

$$\begin{aligned} H_1 &= \xi_2 \\ H_2 &= \xi_2\xi_1 - \xi_0 \\ H_3 &= \xi_0H_2 \end{aligned} \quad (56)$$

The generalized Routh-Hurwitz criterion indicates that \mathcal{E}_* will be locally asymptotically stable if and only if $H_i > 0 \forall i$. This is equivalent to condition (13). Liu [40] also indicates that if

$$H_1 > 0, H_2|_{\alpha_0} = 0, \text{ and } \frac{d}{d\alpha} H_2|_{\alpha_0} \neq 0 \quad (57)$$

thus a necessary condition for a simple Hopf bifurcation to occur is $\xi_0 = \xi_1 \xi_2$. Note condition (57) is equivalent to conditions (14), (15). \square

Proof. (Prop. 6) Existence is clear from the form of \mathcal{E}_c . Note that

$$J(\mathcal{E}_c) = \begin{pmatrix} -\frac{(N_T - c)}{k + N_T - c} & * & \\ 0 & \gamma a(\mathcal{R}_0 - 1) & \end{pmatrix}. \quad (58)$$

\square

Proof. (Prop. 8) The proof is similar to that of Prop. 4 with the difference in detail due only to the Jacobian in the quadratic loss case being:

$$J(\mathcal{E}_*) = \begin{pmatrix} \psi_1 + \psi_2 - \psi_3 - \psi_4 & -az_* & \psi_5 \\ \tilde{\gamma}z_*(\psi_3 - \psi_2) & -a\tilde{\gamma}z_* & 0 \\ -\psi_1 + (1 - \gamma)(\psi_3 - \psi_2) + \psi_4 & az_*(1 - \gamma) & -(\psi_5 + s) \end{pmatrix} \quad (59)$$

and so our characteristic polynomial is

$$\chi_{J(\mathcal{E}_*)}(\lambda) = \lambda^3 + \nu_2 \lambda^2 + \nu_1 \lambda + \nu_0. \quad (60)$$

\square

Proof. (Prop. 9) The proof of dispatavity of model (8) is similar to the proof for such in model (9) (proposition 7). Observe that the Jacobian evaluated at this equilibrium is

$$J(\mathcal{E}'_n) = \begin{pmatrix} \tilde{\epsilon}(\mathcal{P}_0^p - 1) & 0 & 0 & 0 \\ 0 & 0 & 0 & 0 \\ -\frac{\theta}{k + \theta} & 0 & -s & \psi \\ \tilde{\epsilon} & 0 & 0 & -\psi \end{pmatrix} \quad (61)$$

which is block triangular and has eigenvalue $\tilde{\epsilon}(\mathcal{P}_0^p - 1)$ in the p direction. Thus via [34] as in our earlier proofs the desired result follows. \square

Proof. (Prop. 11) First, we observe that since $\mathcal{P}_0^z > 1$ phytoplankton, upon which zooplankton depend, are robustly persistent, and the zooplankton equilibrium \mathcal{E}_{npd}

exists. Next, notice that since a necessary condition for $\mathcal{P}_0^z > 1$ is $\mathcal{R}_{0,1}^z > 1$ it follows that the zooplankton extinction equilibrium is unstable. Next, observe that the eigenvalue in the z direction for this equilibrium is

$$\lambda_z^{\mathcal{E}_{npd}} = b_1(\mathcal{R}_{0,1}^z - 1), \quad (62)$$

(see equation (39)), which is positive whenever $\mathcal{P}_0^z > 1$. Thus as previously (by the work of [34]) zooplankton are robustly persistent, and it follows that there exists at least one coexistence equilibrium. \square

B. Supplementary tables

Table B1: Summary of specific functional forms for the re-scaled system incorporating seasonality and ecological disturbances (model (51))

Functional Form	Description
$1 + \frac{1}{2} \sin(2\pi\tau/100)$	$f_s(\tau)$, Seasonal light availability
$\frac{n}{\bar{k} + n}$	Nutrient uptake rate
$\left(1 - \frac{p}{c}\right)$	Phytoplankton reproduction rate
$\tilde{\epsilon}$	Phytoplankton mortality rate
$\frac{p^2}{1 + p^2}$	Zooplankton grazing rate
$\tilde{\gamma}/f_s(\tau)$	$\tilde{\gamma}_s(\tau)$, zooplankton assimilation rate
$\frac{p^2}{1 + p^2} - \frac{\tilde{\alpha}p}{\xi + p}$	$r(p)$, net zooplankton growth rate
az	Zooplankton mortality rate
$\begin{cases} \theta_d(\tau) &= \theta \pm \frac{M_\theta}{\max_\tau g(\omega, \tau)} g(\omega, \tau) \\ g(\tau) &= \frac{1}{\omega^2} \tau e^{-\tau/\omega}, \end{cases}$	Disturbance function
$\theta(\tau) = \begin{cases} \theta & \tau < \tau_* \\ \theta_d(\tau) & \tau \geq \tau_* \end{cases}$	Intrinsic nutrient level
ψ	Nutrient decay rate

C. Supplementary figures

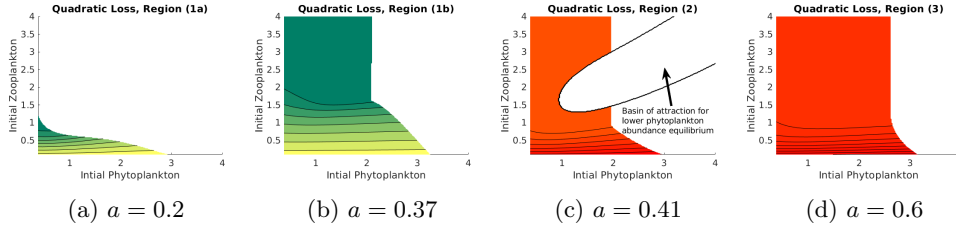


Fig. C1: Bloom occurrence as a function of plankton population at the moment of maximum eutrophication ($\theta = 12$) in the NPZ subsystem at different zooplankton mortality rates using quadratic zooplankton loss term. While other model parameters can change qualitative dynamics, zooplankton loss rate, a is the primary driver of likelihood and type of bloom occurrence, with an implied critical threshold beyond which when a bloom occurs it will be harmful. All other parameter values used are provided in table 2.

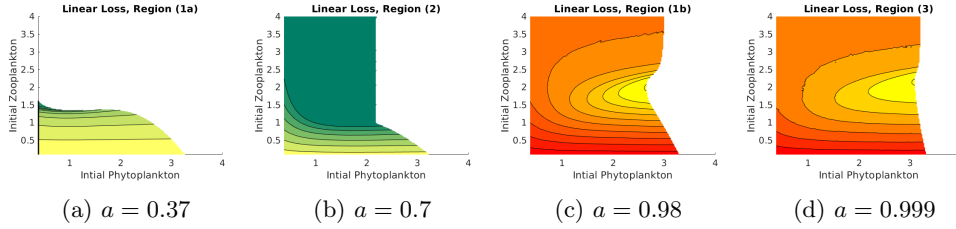


Fig. C2: Bloom occurrence as a function of plankton population at the moment of maximum eutrophication ($\theta = 12$) in the NPZ subsystem at different zooplankton mortality rates using linear zooplankton loss term. The primary difference from the quadratic loss model (Fig. C1) is a much larger zooplankton loss rate to induce different bloom dynamics. While other model parameters can change qualitative dynamics, zooplankton loss rate, a is the primary driver of likelihood and type of bloom occurrence, with an implied critical threshold beyond which when a bloom occurs it will be harmful. All other parameter values used are provided in table 2.

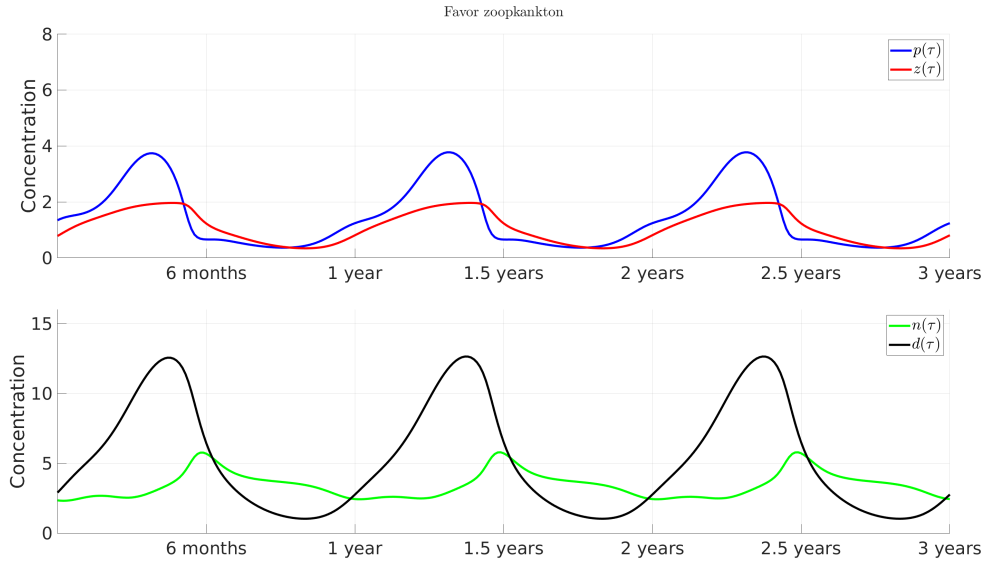


Fig. C3: The model dynamics as a function of ecosystem balance after incorporating seasonality in the region of the parameter space where ecosystem balance favors zooplankton. The parameter values used are: $\tilde{k} = 0.5, c = 10, \tilde{\epsilon} = 0.3, \tilde{\gamma} = 0.29, \tilde{\alpha} = 0.5, \theta = 4, \psi = 0.15, \gamma = 0.5, \xi = 10, a = 0.4, s = 0.3$ (for the unforced model (8), $\mathcal{P}_0^p \approx 3, \mathcal{P}_0^z \approx 5, \mathcal{B} = -0.67$).

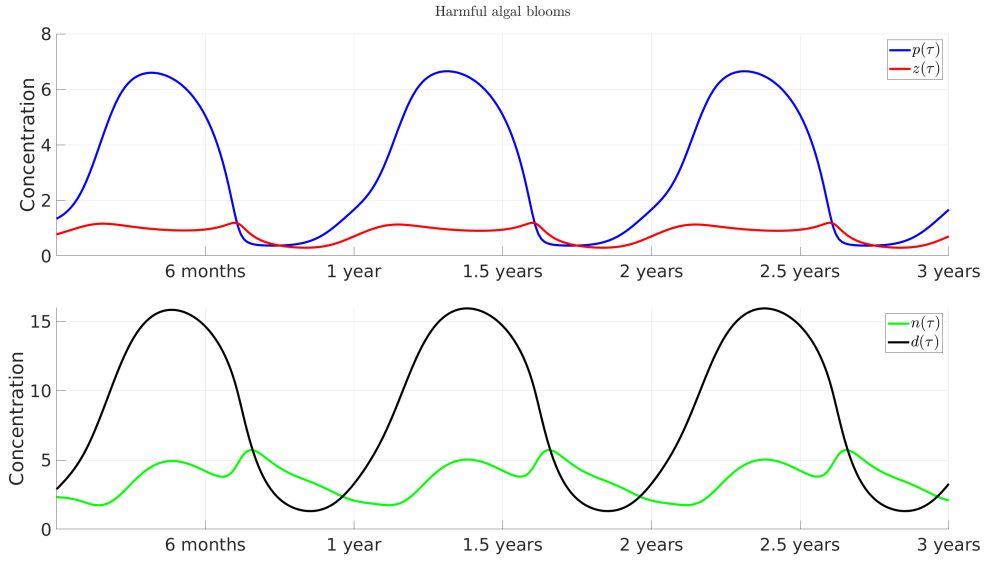


Fig. C4: The model dynamics as a function of ecosystem balance after incorporating seasonality in the region of the parameter space where ecosystem balance favors phytoplankton and HABs occur. The parameter values used are: $\tilde{k} = 0.5, c = 10, \tilde{\epsilon} = 0.3, \tilde{\gamma} = 0.29, \tilde{\alpha} = 1.6, \theta = 4, \psi = 0.15, \gamma = 0.5, \xi = 10, a = 0.4, s = 0.3$ (for the unforced model (8), $\mathcal{P}_0^p \approx 3, \mathcal{P}_0^z \approx 1.5, \mathcal{B} = 0.48$).

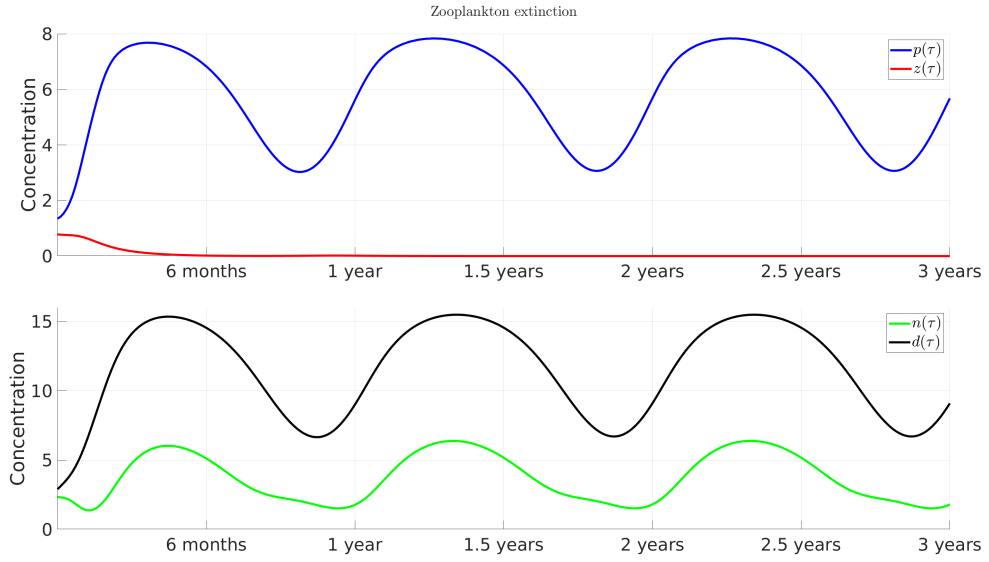


Fig. C5: The model dynamics as a function of ecosystem balance after incorporating seasonality in the region of the parameter space where ecosystem balance favors phytoplankton and zooplankton extinction occurs. The parameter values used are: $\tilde{k} = 0.5$, $c = 10$, $\tilde{\epsilon} = 0.3$, $\tilde{\gamma} = 0.29$, $\tilde{\alpha} = 3.2$, $\theta = 4$, $\psi = 0.15$, $\gamma = 0.5$, $\xi = 10$, $a = 0.4$, $s = 0.3$ (for the unforced model (8), $\mathcal{P}_0^p \approx 3$, $\mathcal{P}_0^z \approx 1.5$, $\mathcal{B} = 0.74$).

References

- [1] Karleskint, G., Turner, R., Small, J.: Introduction to marine biology. Cengage Learning (2012)
- [2] Tittel, J., Bissinger, V., Zippel, B., Gaedke, U., Bell, E., Lorke, A., Kamjunke, N.: Mixotrophs combine resource use to outcompete specialists: implications for aquatic food webs. *Proceedings of the National Academy of Sciences* **100**(22), 12776–12781 (2003)
- [3] Flynn, K.J., Stoecker, D.K., Mitra, A., Raven, J.A., Glibert, P.M., Hansen, P.J., Granéli, E., Burkholder, J.M.: Misuse of the phytoplankton–zooplankton dichotomy: the need to assign organisms as mixotrophs within plankton functional types. *Journal of plankton research* **35**(1), 3–11 (2013)
- [4] Hobbs, R.J., Huenneke, L.F.: Disturbance, diversity, and invasion: implications for conservation. *Conservation Biology* **6**(3), 324–337 (1992)
- [5] Fox, J.W.: The intermediate disturbance hypothesis should be abandoned. *Trends in Ecology & Evolution* **28**(2), 86–92 (2013)
- [6] Richardson, A.J.: In hot water: zooplankton and climate change. *J. Mar. Sci* **65**, 279–295 (2008)
- [7] Barton, A.D., Irwin, A.J., Finkel, Z.V., Stock, C.A.: Anthropogenic climate change drives shift and shuffle in north atlantic phytoplankton communities. *Proceedings of the National Academy of Sciences* (2016) <https://doi.org/10.1073/pnas.1519080113>
<https://www.pnas.org/content/early/2016/02/17/1519080113.full.pdf>
- [8] Chust, G., Vogt, M., Benedetti, F., Nakov, T., Villéger, S., Aubert, A., Vallina, S.M., Righetti, D., Not, F., Biard, T., Gaborit, C., Cornils, A., Buttay, L., Irisson, J.-O., Chiarello, M., Vallim, A.L., Blanco-Bercial, L., Basconi, L., Ayata, S.-D.: Mare incognitum: A glimpse into future plankton diversity and ecology research. *Frontiers in Marine Science* **4**, 68 (2017)
- [9] Hallegraeff, G.M.: A review of harmful algal blooms and their apparent global increase. *Phycologia* **32**(2), 79–99 (1993)
- [10] Anderson, D.M., Gilbert, P.M., Burkholder, J.M.: Harmful algal blooms and eutrophication: Nutrient sources, composition, and consequences. *Estuaries* **25**, 704–726 (2002)
- [11] Ibáñez, C., Peñuelas, J.: Changing nutrients, changing rivers. *Science* **365**(6454), 637–638 (2019)
- [12] Trubovitz, S., Lazarus, D., Renaudie, J., Noble, P.J.: Marine plankton show threshold extinction response to neogene climate change. *Nature communications*

11(1), 1–10 (2020)

- [13] Hilborn, E.D., Roberts, V.A., Backer, L., DeConno, E., Egan, J.S., Hyde, J.B., Nicholas, D.C., Wiegert, E.J., Billing, L.M., DiOrio, M., *et al.*: Algal bloom-associated disease outbreaks among users of freshwater lakes-united states, 2009–2010. *Morbidity and Mortality Weekly Report* **63**(1), 11 (2014)
- [14] Kouakou, C.R., Poder, T.G.: Economic impact of harmful algal blooms on human health: a systematic review. *Journal of water and health* **17**(4), 499–516 (2019)
- [15] Lassudrie, M., Hegaret, H., Wikfors, G.H., Silva, P.M.: Effects of marine harmful algal blooms on bivalve cellular immunity and infectious diseases: A review. *Developmental & Comparative Immunology* **108**, 103660 (2020)
- [16] Hu, H., Zhang, J., Chen, W.: Competition of bloom-forming marine phytoplankton at low nutrient concentrations. *Journal of Environmental Sciences* **23**(4), 656–663 (2011)
- [17] Anderson, T.H., Taylor, G.T.: Nutrient pulses, plankton blooms, and seasonal hypoxia in western long island sound. *Estuaries* **24**(2), 228–243 (2001)
- [18] Diaz, R.J.: Overview of hypoxia around the world. *Journal of environmental quality* **30**(2), 275–281 (2001)
- [19] Sylvan, J.B., Dortch, Q., Nelson, D.M., Maier Brown, A.F., Morrison, W., Ammerman, J.W.: Phosphorus limits phytoplankton growth on the louisiana shelf during the period of hypoxia formation. *Environmental science & technology* **40**(24), 7548–7553 (2006)
- [20] Ralston, D.K., Moore, S.K.: Modeling harmful algal blooms in a changing climate. *Harmful Algae* **91**, 101729 (2020)
- [21] Carstensen, J., Henriksen, P., Heiskanen, A.-S.: Summer algal blooms in shallow estuaries: Definition, mechanisms, and link to eutrophication. *Limnology and Oceanography* **52**(1), 370–384 (2007) <https://doi.org/10.4319/lo.2007.52.1.0370>
<https://aslopubs.onlinelibrary.wiley.com/doi/pdf/10.4319/lo.2007.52.1.0370>
- [22] Mackas, D.L., Denman, K.L., Abbott., M.R.: Complete global analysis of a diffusive npz model with age structure in zooplankton. *Bulletin of Marine Science* **37**(2), 652–674 (1985)
- [23] Busenberg, S., Kumarand, S.K., Austin, P., Wake, G.: The dynamics of a model of a plankton-nutrient interaction. *Bulletin of Mathematical Biology* **52**(5), 677–696 (1990)
- [24] Steele, J.H., Henderson, E.W.: The role of predation in plankton models. *Journal of Plankton Research* **14**(1), 157–172 (1992)

- [25] Edwards, A.M., Yool, A.: The role of higher predation in plankton population models. *Journal of Plankton Research* **22**(6), 1085–1112 (2000)
- [26] Edwards, A.M.: Adding detritus to a nutrient–phytoplankton–zooplankton model: a dynamical-systems approach. *Journal of Plankton Research* **23**(4), 389–413 (2001)
- [27] Franks, P.J.S.: Npz models of plankton dynamics: Their construction, coupling to physics, and application. *Journal of Oceanography* **58**, 379–387 (2002)
- [28] Heinle, A., Slawig, T.: Internal dynamics of npzd type ecosystem models. *Ecological Modeling* **254**, 33–42 (2013)
- [29] Kloosterman, M., Campbell, S.A., Poulin, F.J.: A closed npz model with delayed nutrient recycling. *Journal of Mathematical Biology* **68**, 815–850 (2014)
- [30] Holling, C.S.: The components of predation as revealed by a study of small-mammal predation of the european pine sawfly. *The Canadian Entomologist* **91**(5), 293–320 (1959)
- [31] Gulbudak, H., Browne, C.J.: Infection severity across scales in multi-strain immuno-epidemiological dengue model structured by host antibody level. *Journal of mathematical biology* **80**(6), 1803–1843 (2020)
- [32] Andronov, A.A.: *Theory of Bifurcations of Dynamic Systems on a Plane*. Israel Program for Scientific Translations, Jerusalem (1971)
- [33] Smith, H.L., Thieme, H.R.: *Dynamical Systems and Population Persistence*. American Mathematical Society, Providence, Rhode Island (2011)
- [34] Salceanu, P.L.: Robust uniform persistence in discrete and continuous dynamical systems using lyapunov exponents. *Mathematical Biosciences and Engineering* **8**(3), 807–825 (2011)
- [35] Macdonald, J.C., Gulbudak, H.: Software for Forward hysteresis and Hopf bifurcation in a NPZD model with application to harmful algal blooms. Zenodo (2023). <https://doi.org/10.5281/zenodo.7650342>
- [36] Gulbudak, H., Martcheva, M.: Forward hysteresis and backward bifurcation caused by culling in an avian influenza model. *Mathematical biosciences* **246**(1), 202–212 (2013)
- [37] Scheffer, M., Carpenter, S., Foley, J.A., Folke, C., Walker, B.: Catastrophic shifts in ecosystems. *Nature* **413**(6856), 591–596 (2001)
- [38] Scheffer, M., Bascompte, J., Brock, W.A., Brovkin, V., Carpenter, S.R., Dakos, V., Held, H., Van Nes, E.H., Rietkerk, M., Sugihara, G.: Early-warning signals for critical transitions. *Nature* **461**(7260), 53–59 (2009)

- [39] Scheffer, M., Carpenter, S.R., Lenton, T.M., Bascompte, J., Brock, W., Dakos, V., Koppel, J., Leemput, I.A., Levin, S.A., Van Nes, E.H., *et al.*: Anticipating critical transitions. *science* **338**(6105), 344–348 (2012)
- [40] Liu, M.W.: Criterion of hopf bifurcations without using eigenvalues. *Journal of Mathematical Analysis and Applications* **182**, 250–256 (1994)